Lymphoma

LYMPHOMA

ANTHONY A. MANCUSO

KEY POINTS

- Lymphoma is a common disease of the head and neck.
- Lymphoma most often presents as nodal disease.
- In its extranodal varieties, it takes on appearances that mimic other pathologies.
- Angiocentric and angiotropic lymphoma are forms that may commonly be mistaken for other pathology.
- Differentiation of lymphoma from reactive or proliferative but benign lymphoid processes is often difficult based on imaging findings.

INTRODUCTION

Prevalence and Etiology

Lymphoma is a relatively common malignancy of uncertain precise etiology. It has associations with disorders such as HIV and Epstein-Barr virus infection but no definitive causative relationship.[1,2] The disease affects all age groups but is most common in young to middle-aged adults.[3]

In general, it is difficult to determine the frequency of lymphoma arising primarily in, or strictly limited to, the head and neck region. Often, head and neck lymphoma is part of systemic involvement. However, the head and neck region may be the site of presenting complaints in secondary as well as primary disease. The best known presentation is probably cervical adenopathy; however, lymphoma can mimic most infiltrating highly cellular malignancies at any particular site. It is probably best to also consider the chronic leukemias in this context from a morphologic and spread pattern perspective since their nodal presentation cannot be distinguished from lymphoma, but these are not lymphomas and not part of the classification. The nodal expression of this disease is considered in more detail in conjunction with reactive and lymphomatous lymphadenopathy in Chapter 158.

The patterns of disease spread described in the following material will apply across lymphoma that involves in all anatomic regions of the head and neck.

PATTERNS OF DISEASE AND PATHOLOGY

The debate of how to classify lymphomas is well beyond the scope of this text. For a simple and reasonable approach, the fundamental separation of types used by the Lukes-Collins Revised Classification and Revised European-American Lymphoma (REAL) Classification is used here. The non-Hodgkin types are separated into T-cell and B-cell groups. Hodgkin disease is then the third major group.

Almost all of these diseases express themselves in the head and neck region often just as nodal disease. Some, like the chronic leukemias and Hodgkin disease, present almost entirely as nodal disease. Many also involve extranodal sites. It is the extranodal disease that is often most challenging to diagnosis correctly since the variable sites, morphology, and propensity for perineural and perivascular spread of some types of lymphoma make its presentation at extranodal sites protean.[4] For this reason, lymphoma should enter the differential diagnosis of an infiltrating process in the head and neck when the disease morphology appears “unusual” for want of a better term or the pattern is multifocal and possibly perineural and perivascular (Figs. 27.1 and 27.2).

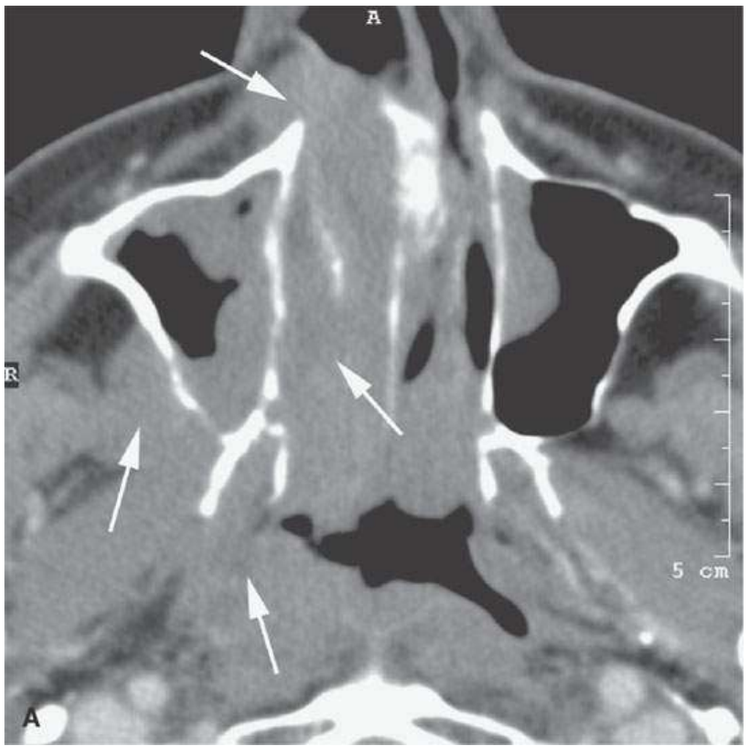
A
R
5 cm
A

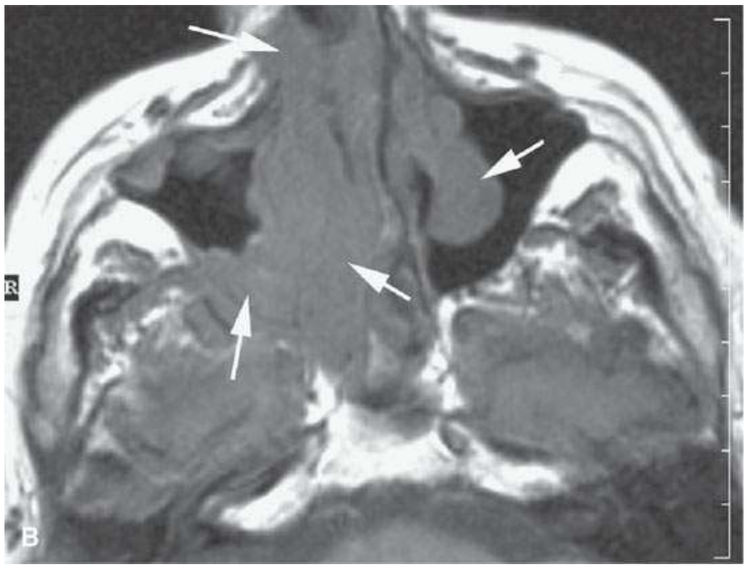
R
B

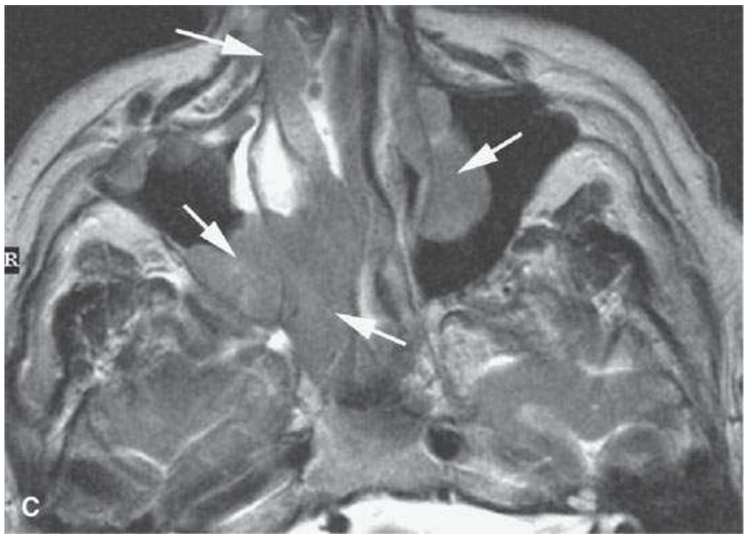
R
C

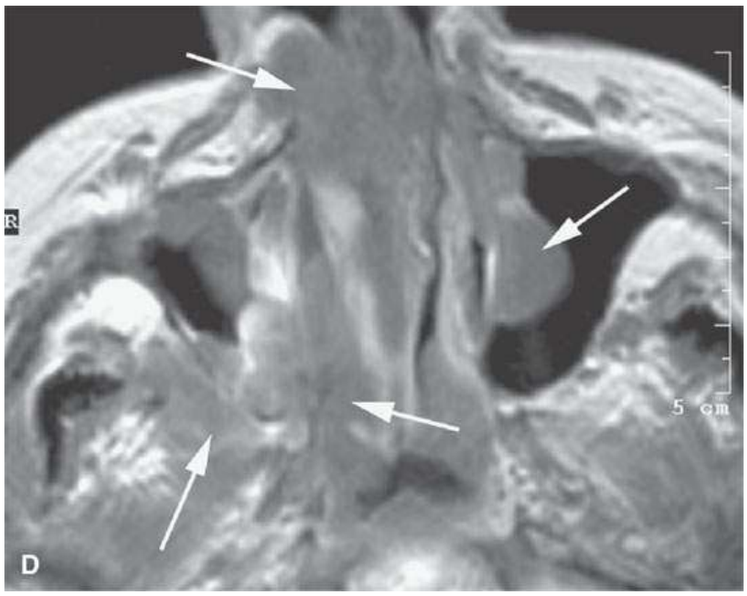

FIGURE 27.1. Contrast-enhanced computed tomography (CECT) and magnetic resonance imaging in a patient presenting with nasal stuffiness. Both studies show a multifocal, bilateral minimally enhancing mass not only of the sinuses and nasal cavity but also of the infratemporal fossa and nasopharynx *(arrows)*. **A:** CECT. **B:** Non–contrast-enhanced T1-weighted (T1W) image. **C:** T2-weighted image. **D:** Contrast-enhanced T1W image.

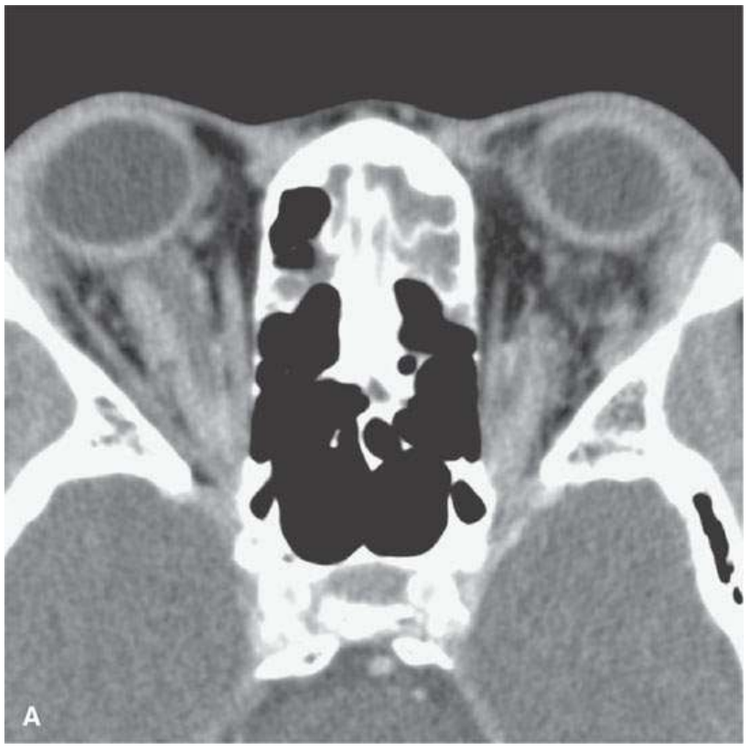

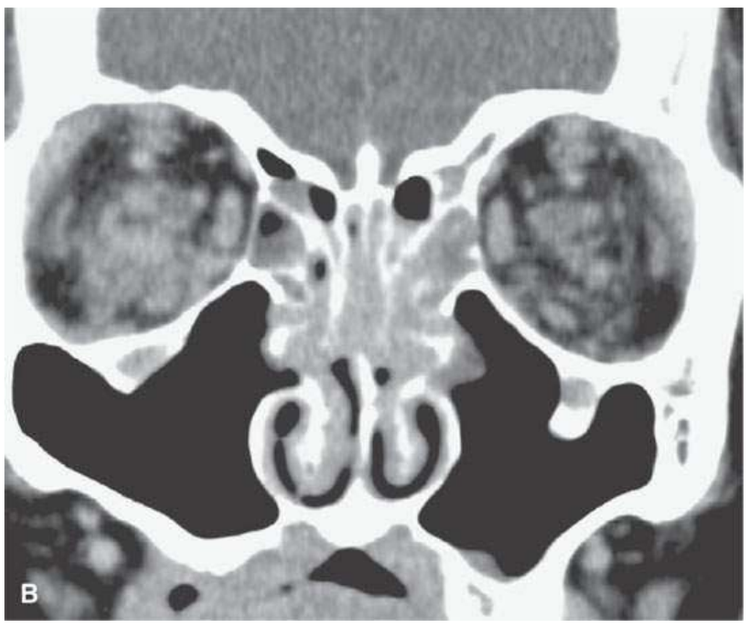

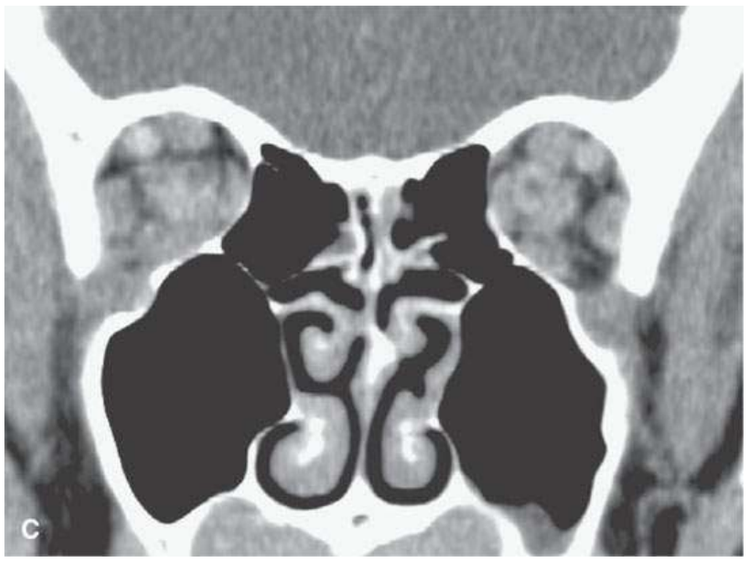
C

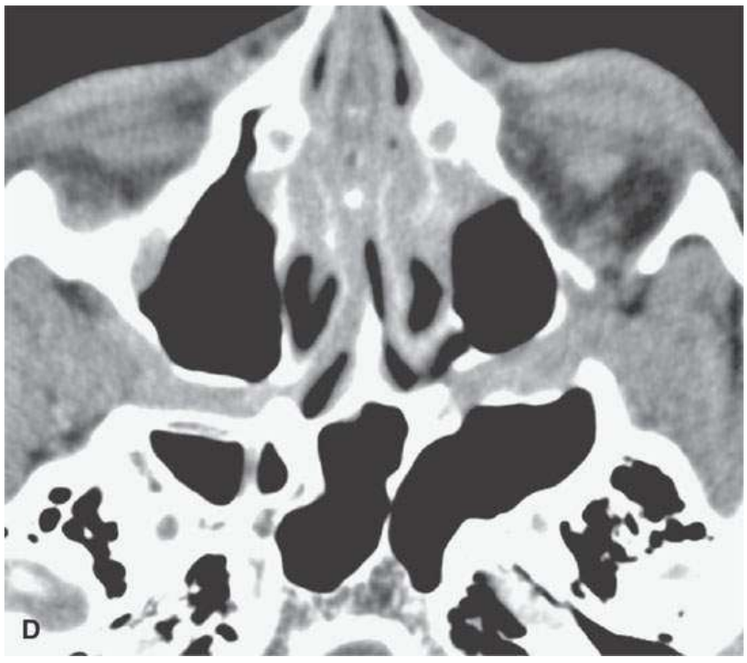
D

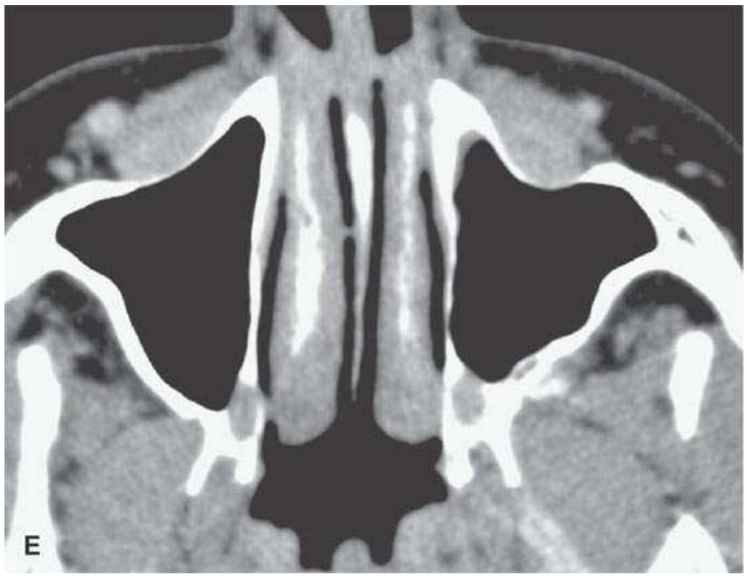
E

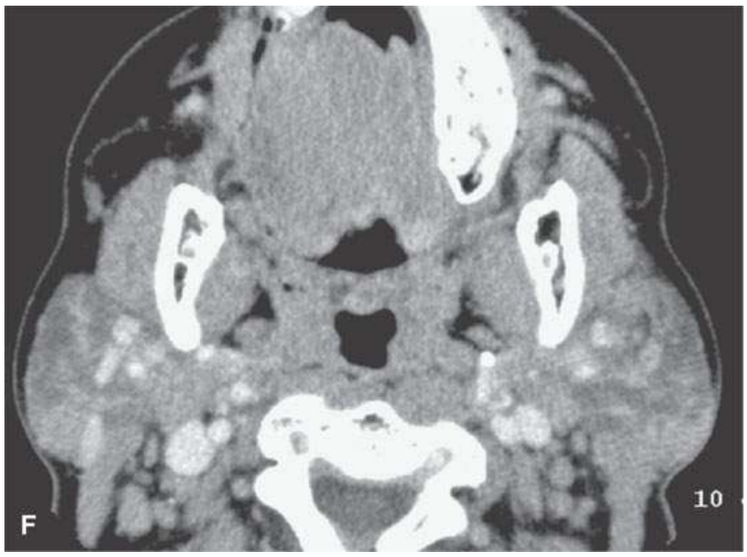

FIGURE 27.2. Contrast-enhanced computed tomography showing a minimally enhancing multifocal, bilateral infiltrating process in the orbits **(A–C)**, nasal cavity **(B)**, showing avidity for perineural spread along the infraorbital nerve canals **(B, C)**, in the pterygopalatine fossa **(D)**, and beneath the superficial musculoaponeurotic system **(E).** The parotid glands are involved bilaterally as well **(F)**.

Immunocytochemical phenotyping and molecular genetics have altered the management of lymphoma and related necrotizing sinonasal diseases discussed in Chapter 92 as well as their differentiation from diseases such as Wegener granulomatosis or sarcoidosis. Terms like *polymorphic reticulosis* and *lymphomatoid granulomatosis* are also no longer used. The majority of these previously pathologically poorly understood entities are now known to be sinonasal lymphomas of B-cell lymphoma, T-cell lymphoma, and natural killer (NK)/T-cell lymphoma with a broad range of biologic activity depending on their immunophenotype. NK/T-cell lymphoma is strongly associated with the Epstein-Barr virus. The locoregional failure rates in these tumors are similar; however, distant failure is much more common in B-cell or NK/T-cell lymphoma than in T-cell lymphoma. T-cell lymphoma has the most favorable prognosis, and NK/T-cell has the worst.

Extranodal Disease Trends in B-Cell Lymphoma

In general, the extranodal sites of interest include the lacrimal glands (Fig. 27.3) and other contents of the orbits (Figs. 27.2 and 27.4), nasal cavity and sinuses (Fig. 27.5), the parotid glands (Figs. 27.6 and 27.7), the Waldeyer ring (Figs. 27.8 and 27.9), and thyroid gland (Fig. 27.10). Unusual sites of presentation include the canine fossa of the cheek, the buccal space, and the infratemporal fossa likely due to at least some relationship to the facial nodes and related lymphoid elements in these locations (Figs. 27.2 and 27.11), as discussed in Chapter 149. Disease in the larynx and trachea is rare (Figs. 27.12). As an example of potential uniqueness in an area where things tend to look the same, Burkitt lymphoma may be the most readily recognizable B-cell lymphoma due to its predilection for the facial bones and, particularly, the mandible (Fig. 27.13). Burkitt lymphoma also has both an extraordinary growth rate and an equally extraordinary tendency to respond quickly to chemotherapy.

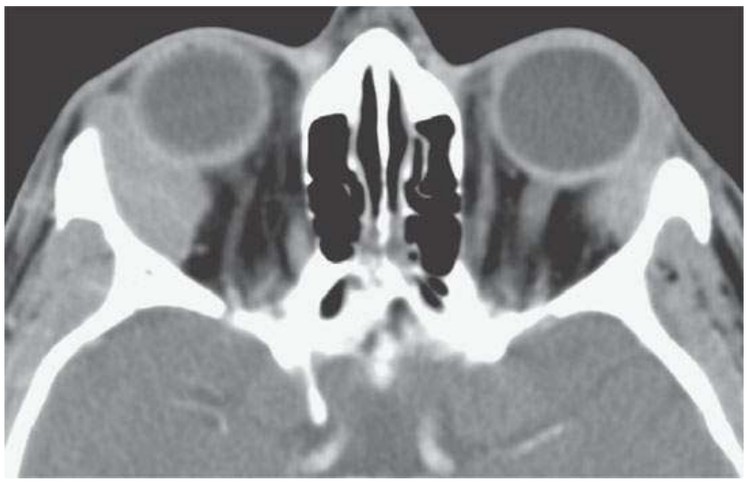

FIGURE 27.3. Contrast-enhanced computed tomography of lacrimal gland lymphoma. At this time, the patient had no systemic disease.

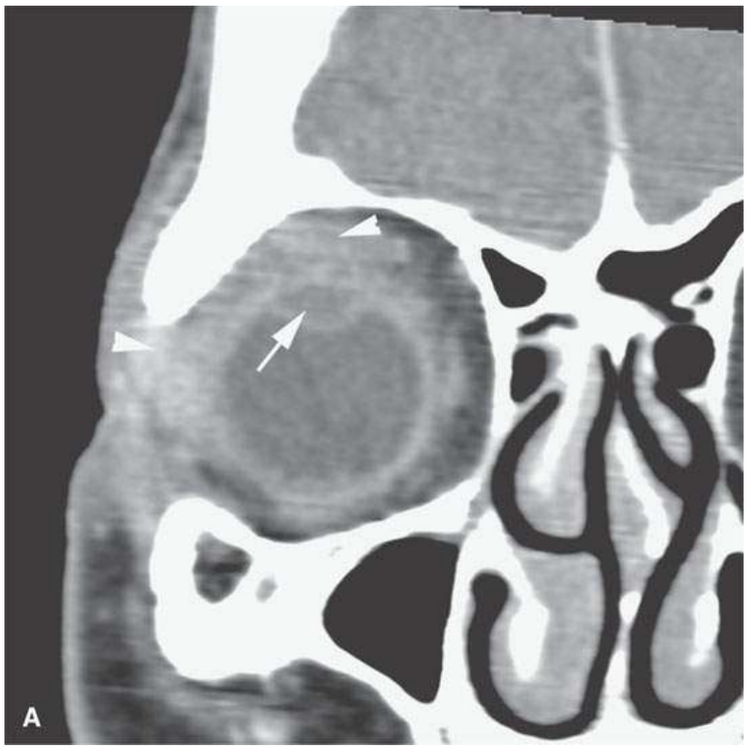

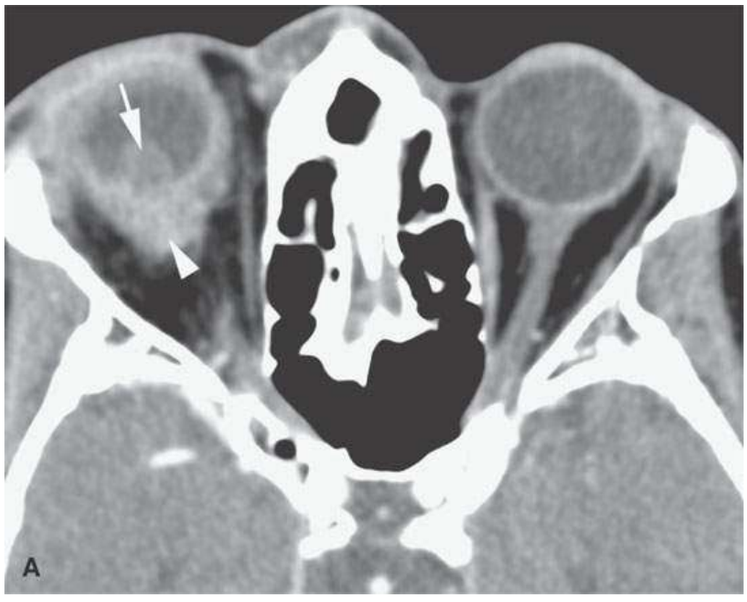

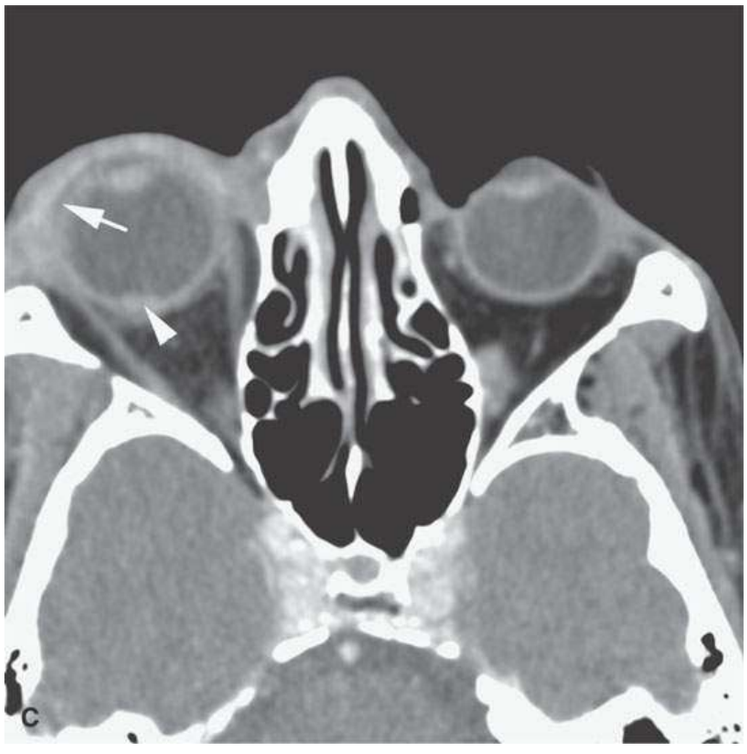

FIGURE 27.4. Contrast-enhanced computed tomography of a patient with a particularly unusual pattern of orbital lymphoma *(arrowheads)* with ocular invasion *(arrows)*.

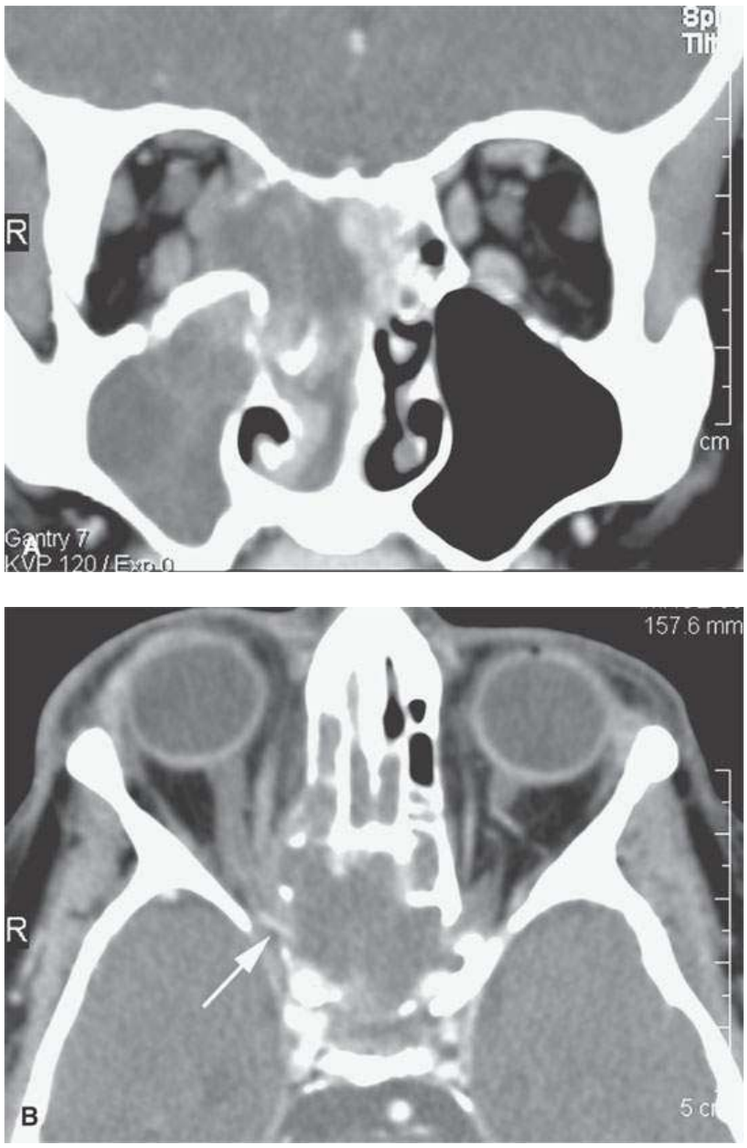

FIGURE 27.5. Contrast-enhanced computed tomography of primary sinonasal lymphoma with orbital invasion and spread to the orbital apex (*arrow* in **B**) threatening optic nerve function.

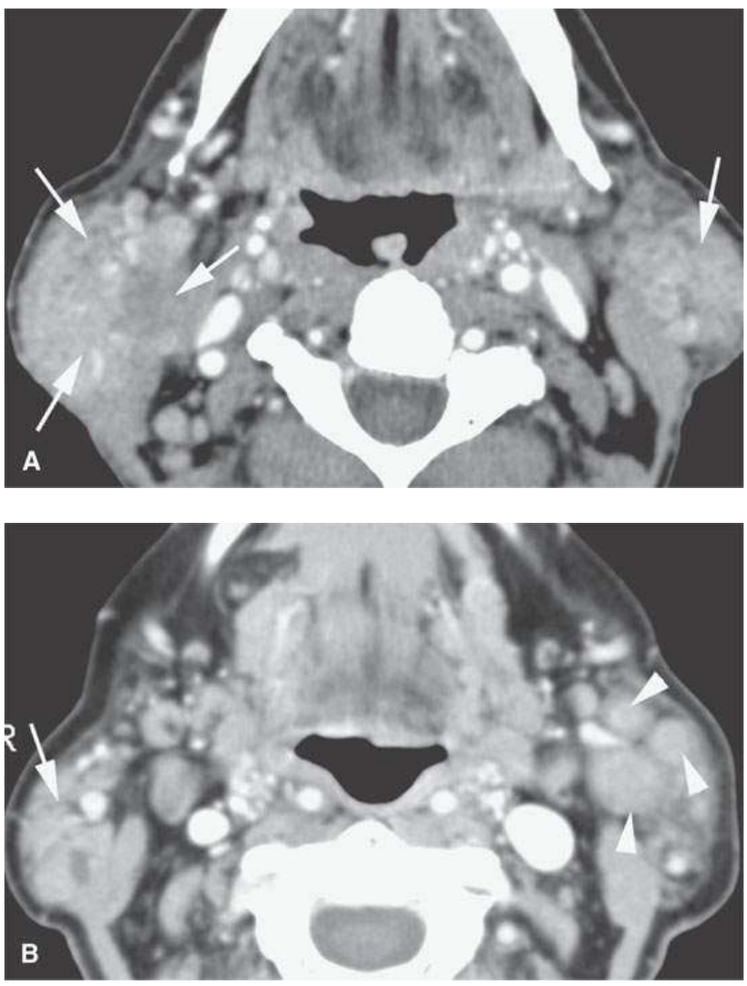

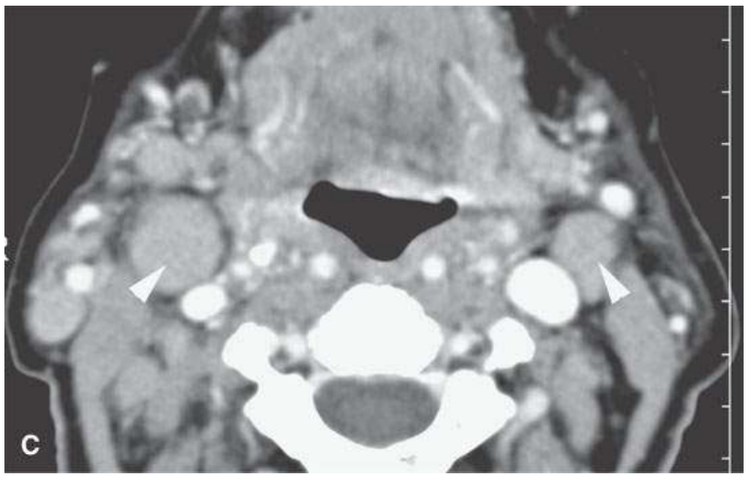

FIGURE 27.6. Contrast-enhanced computed tomography and magnetic resonance imaging studies of a patient with long-standing Sjögren disease with a secondary lymphoma. **A–C:** Confluent masses showed progressive enlargement on serial studies *(arrows)*. Confluent masses are not necessarily due to lymphoma in this setting; however, the nodal enlargement *(arrowheads)* prompted biopsy to reveal lymphoma.

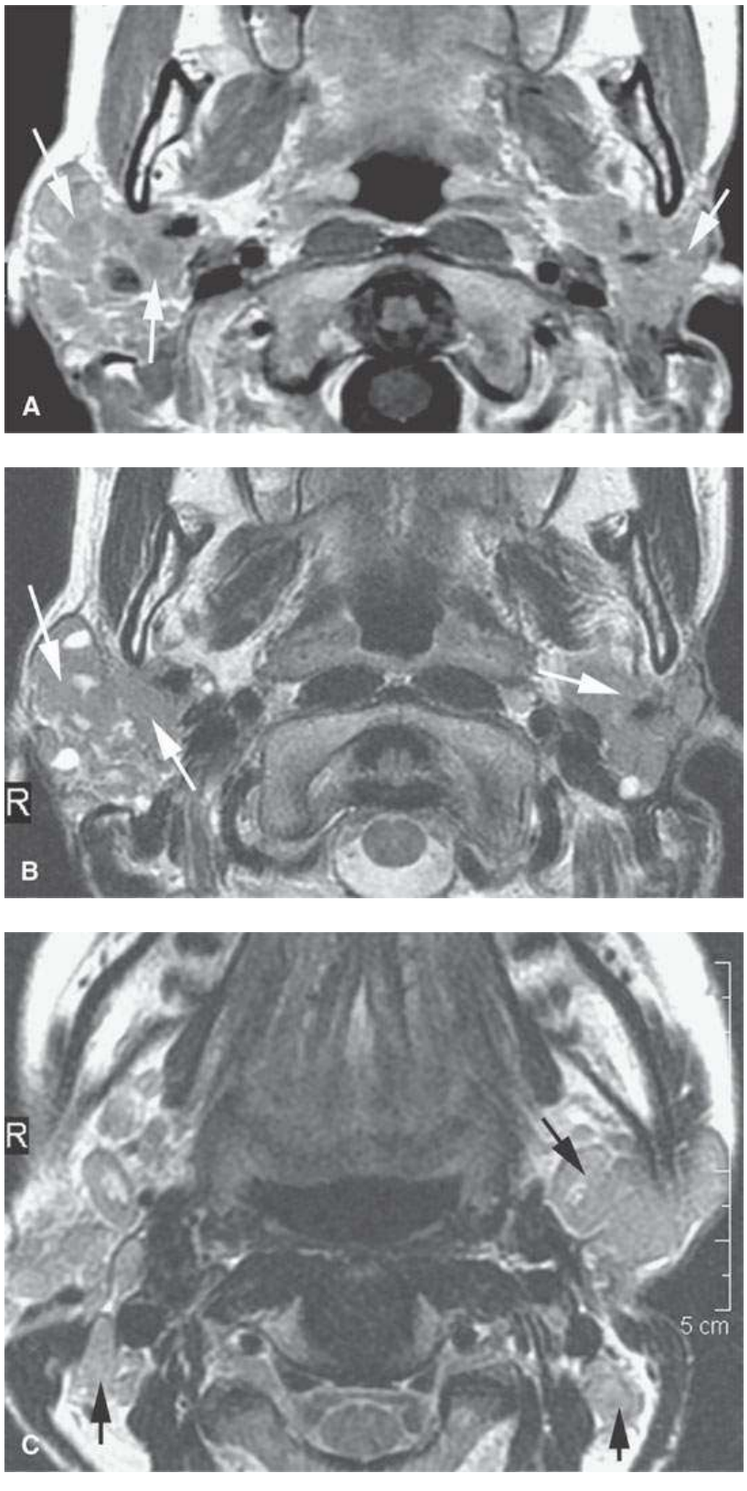

FIGURE 27.7. Magnetic resonance imaging studies of a patient with long-standing Sjögren disease with a secondary lymphoma. **A–C:** Confluent masses showed progressive enlargement on serial studies *(arrows)*. Confluent masses are not necessarily due to lymphoma in this setting; however, their progressive enlargement *(arrowheads)* prompted biopsy to reveal lymphoma. **A:** Contrast-enhanced T1-weighted image. **B, C:** T2-weighted images.

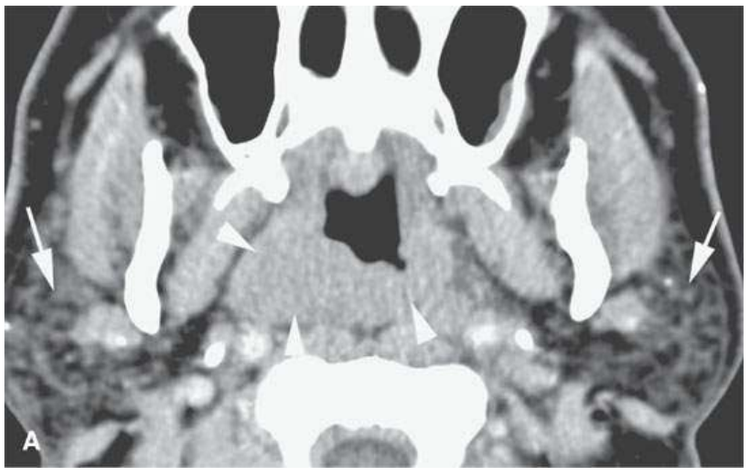

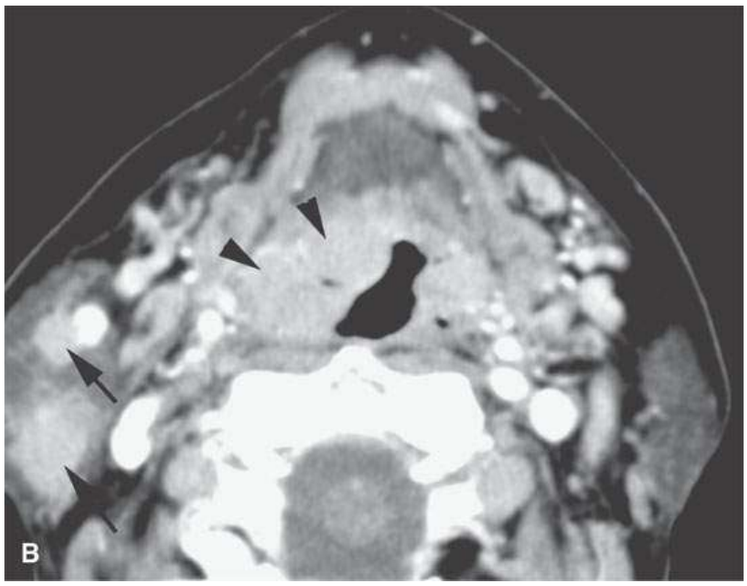

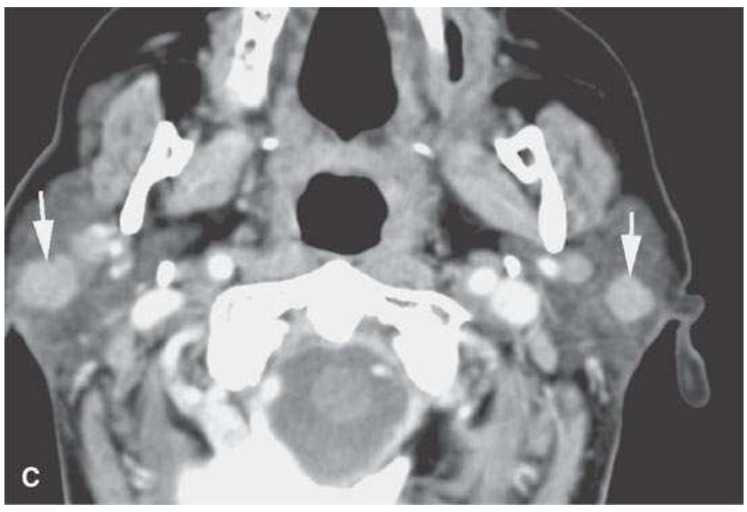

FIGURE 27.8. Contrast-enhanced computed tomography (CT) of a patient with long-standing Sjögren disease *(arrows* in **A**) with a secondary lymphoma**.** The patient developed some suspicious adenopathy clinically leading to this CT**. A–C**: CT showed an infiltrating mass in the nasopharynx *(arrowheads* in **A**) and oropharynx **(B)** in the lymphoid tissue of the Waldeyer ring *(arrowheads)***.** Enlargement of parotid nodes *(arrowheads)was* also present *(arrows* in **B and C**)**.** The findings prompted biopsy that confirmed lymphoma**.**

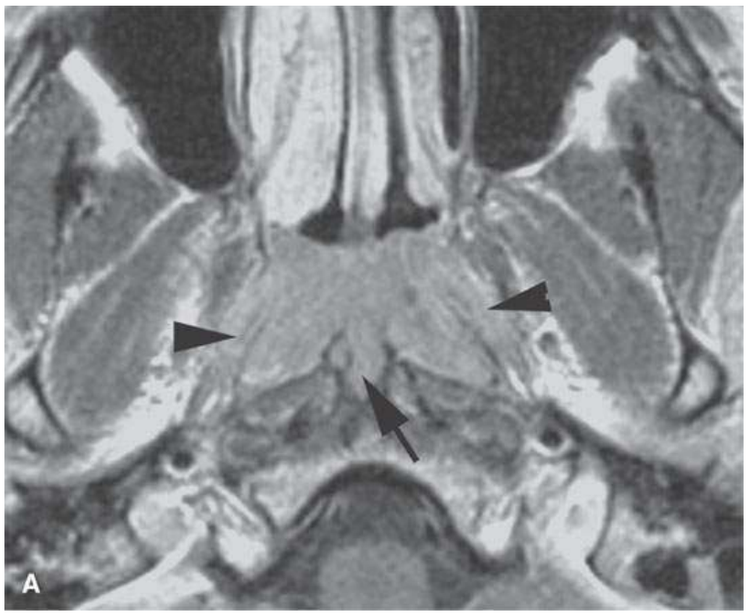
A

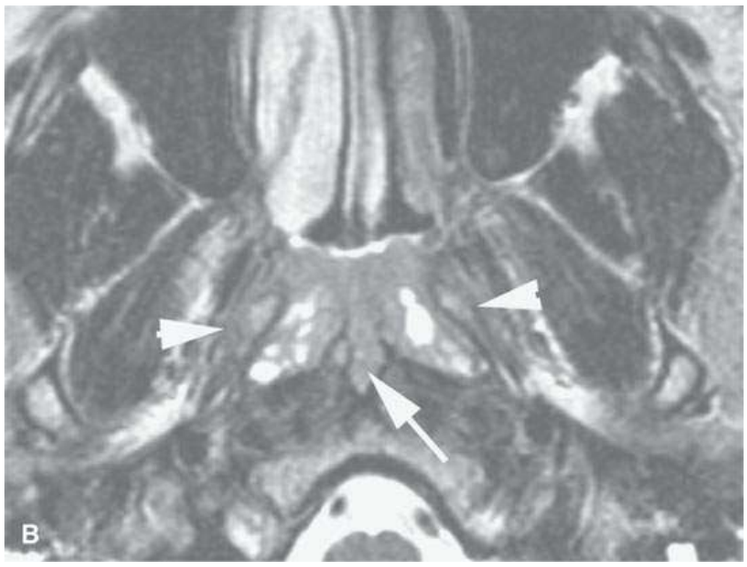
B

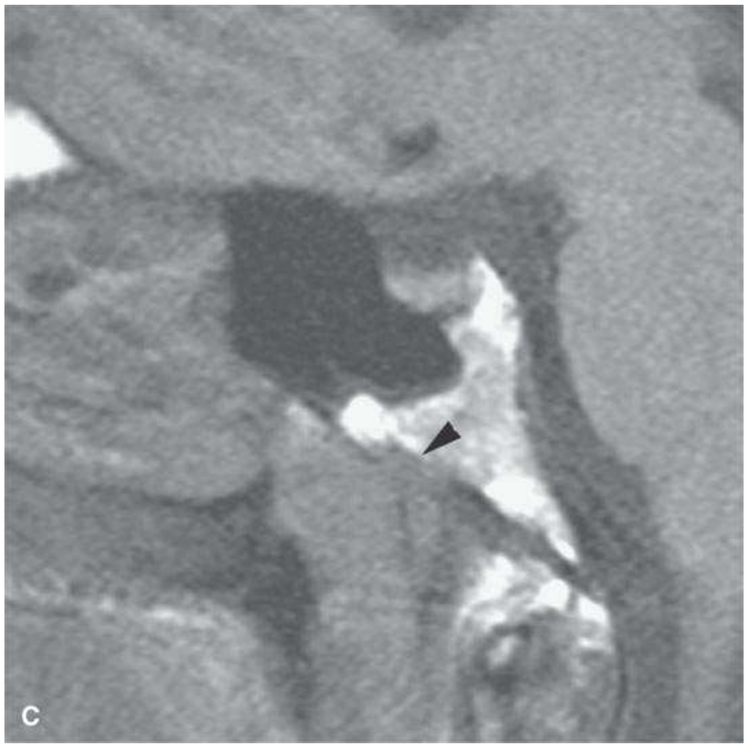
C

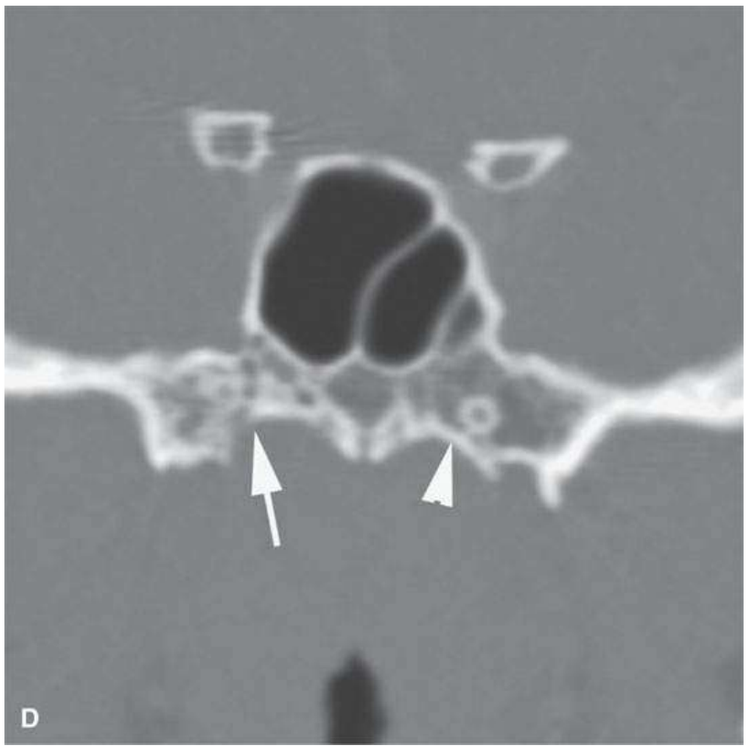

FIGURE 27.9. Contrast-enhanced magnetic resonance demonstrating early infiltrating lymphoma of the nasopharynx**. A:** Contrast-enhanced T1-weighted (T1W) image shows early infiltration of the parapharyngeal fat and palatal musculature *(arrowheads)* that border the nasopharynx, suggesting early clival invasion *(arrow)***. B:** T2-weighted image correlating with **(A)** confirms those findings**. C:** Non–contrast-enhancedT1W image suggest early clival erosions *(arrow)***. D:** Computed tomography confirms early cortical bone erosion just to the right of midline *(arrow)* compared to the normal cortex just to the left of midline *(arrowhead)***.**

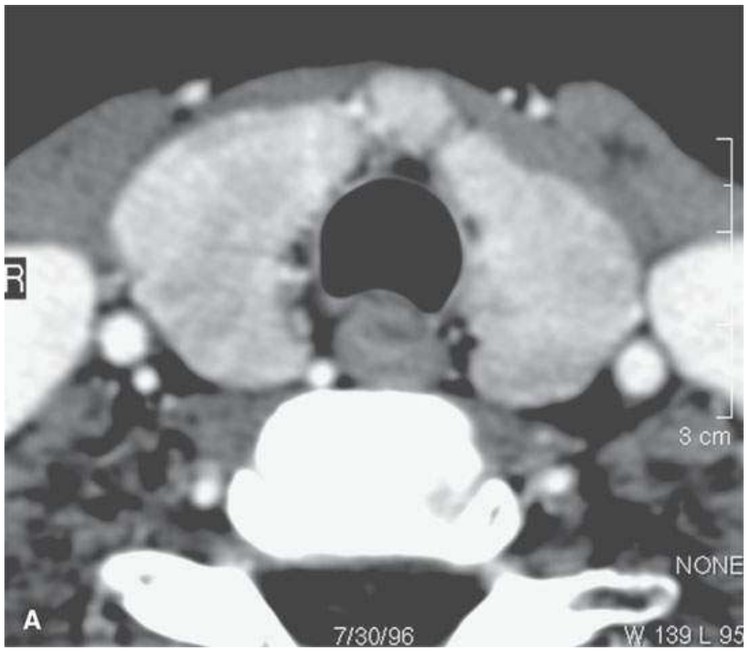

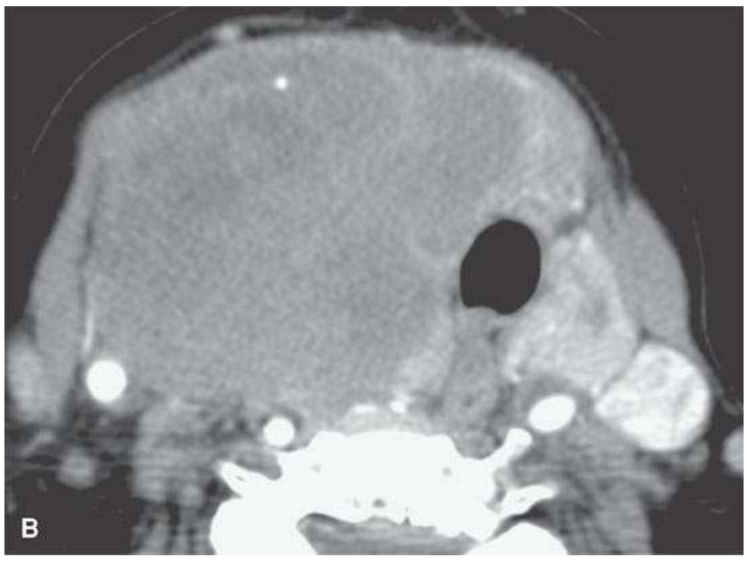

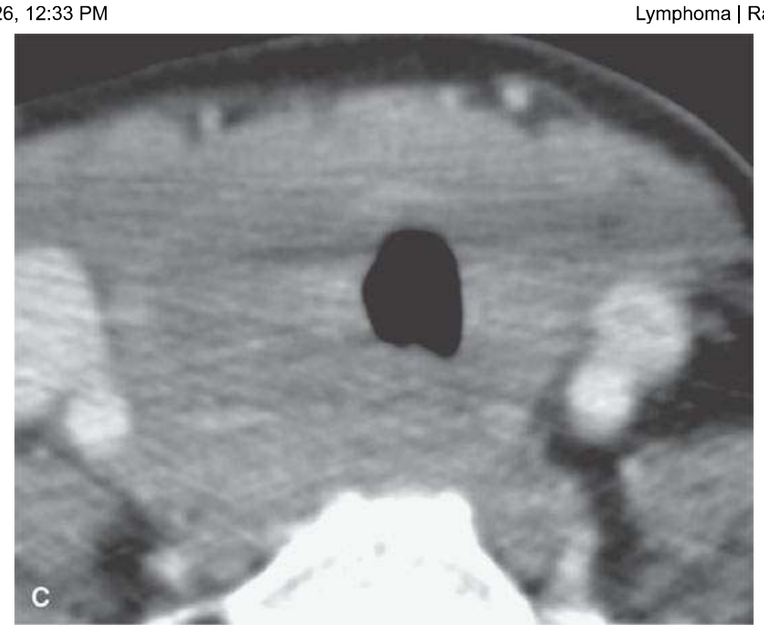

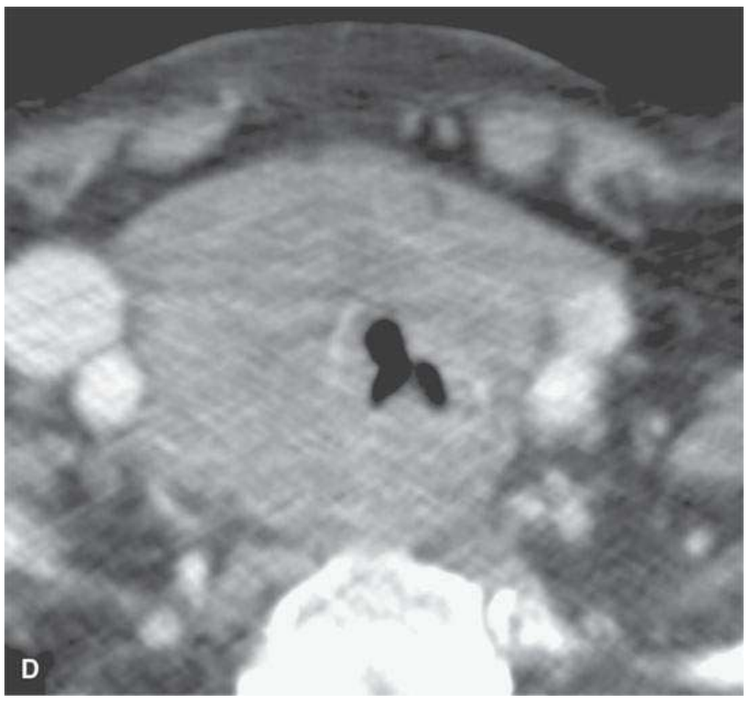

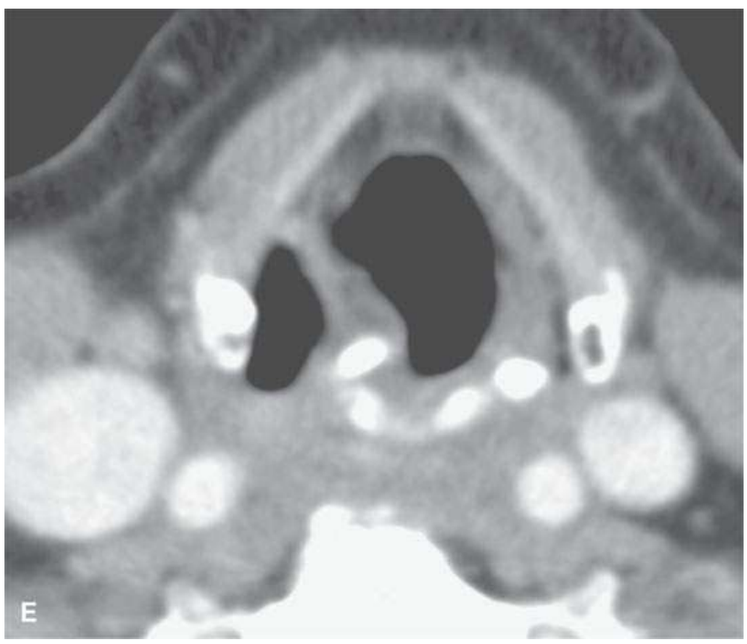

FIGURE 27.10. Contrast-enhanced computed tomography studies of four patients with thyroid lymphoma of various degrees of involvement of the gland and surrounding structures. A;: Bilateral symmetric gland enlargement essentially indistinguishable form other causes of generalized glandular hyperplasia. **B**: Unilateral enlargement with early spread beyond the gland capsule in a pattern that would also suggest anaplastic carcinoma. C : Diffuse enlargement with extensive spread beyond the gland capsule in a pattern that would also suggest anaplastic carcinoma. **D**, **E**: The potential for airway compromise **(D)** and compromise of adjacent nerves manifest here as true vocal cord weakness **(E).**

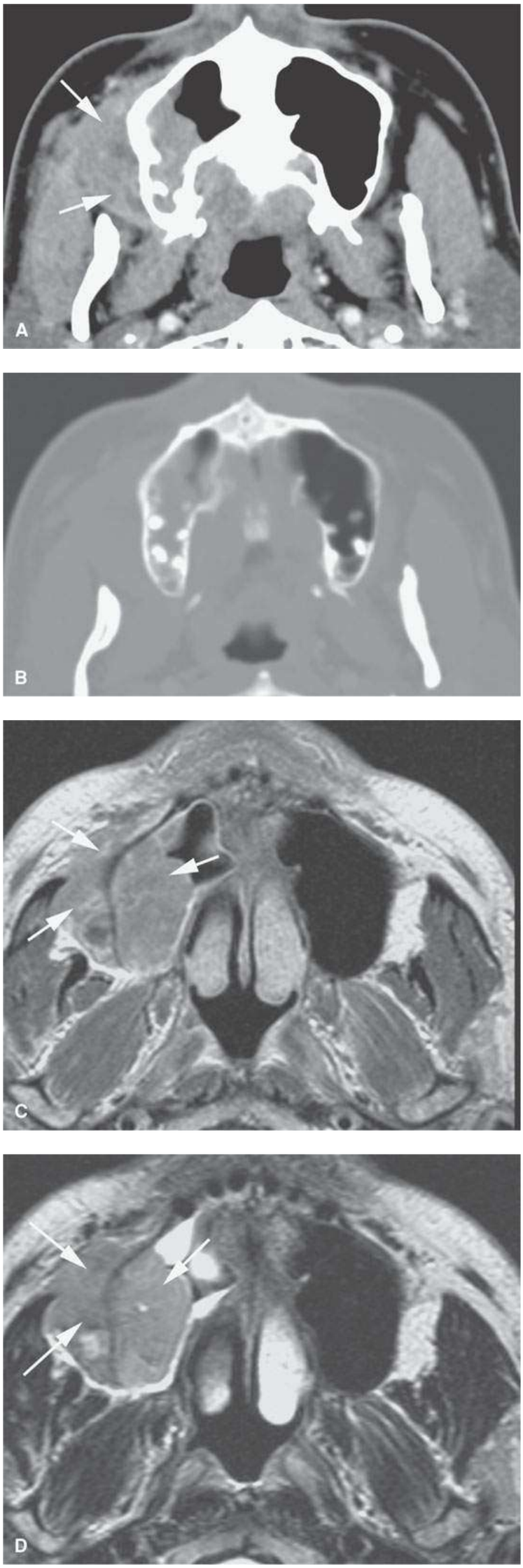

FIGURE 27.11. Contrast-enhanced computed tomography (CECT) and magnetic resonance imaging in a patient with MALT lymphoma**.** The tumor *(arrows)* was primary in the region of the maxillary infrastructure and upper gingival buccal sulcus**. A, B:** CECT**. C:** Contrast-enhancedT1-weighted image**. D:** T2-weighted

image.

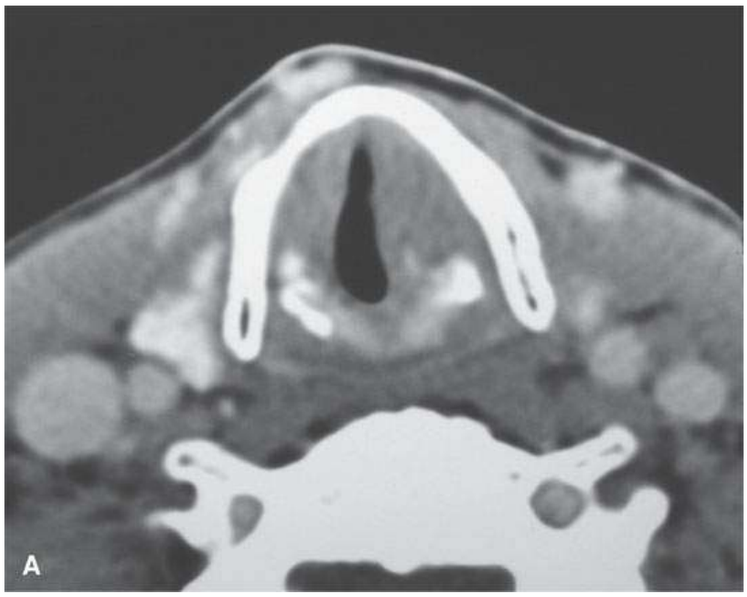

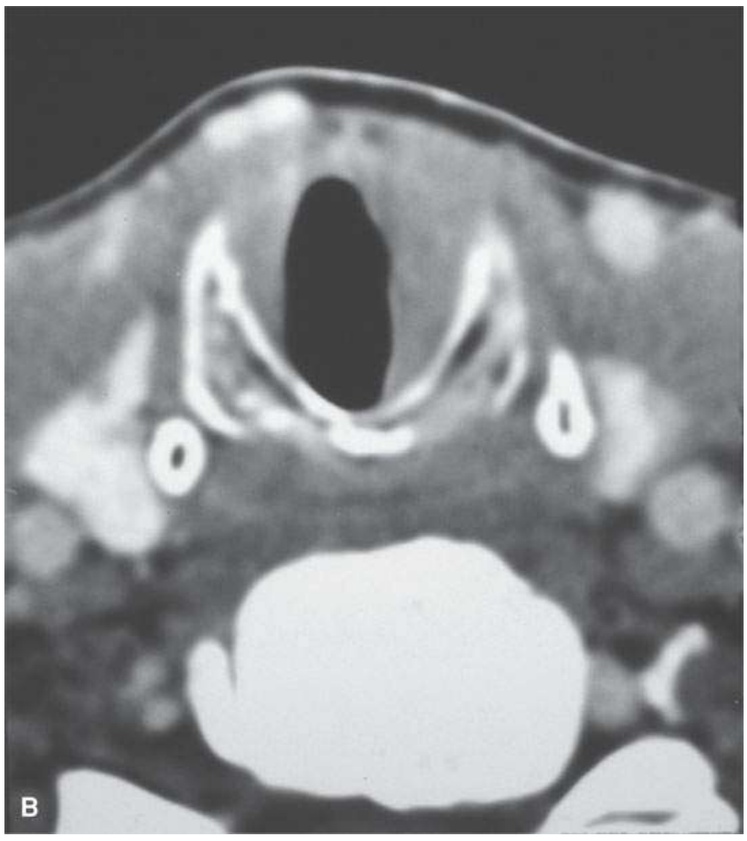

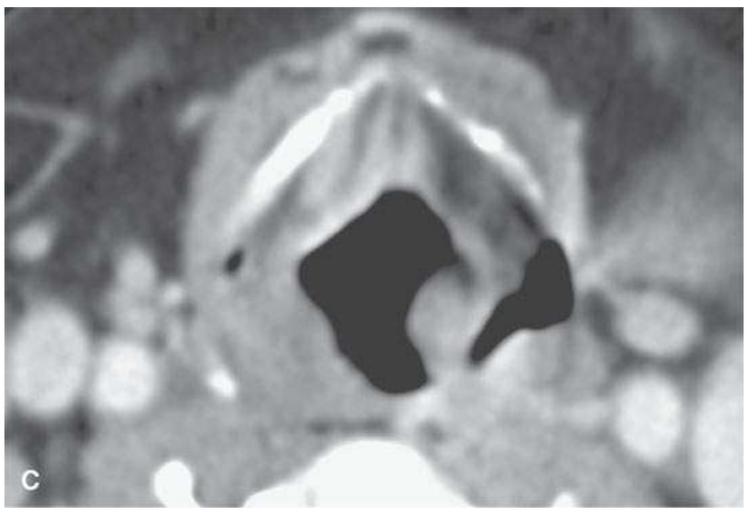

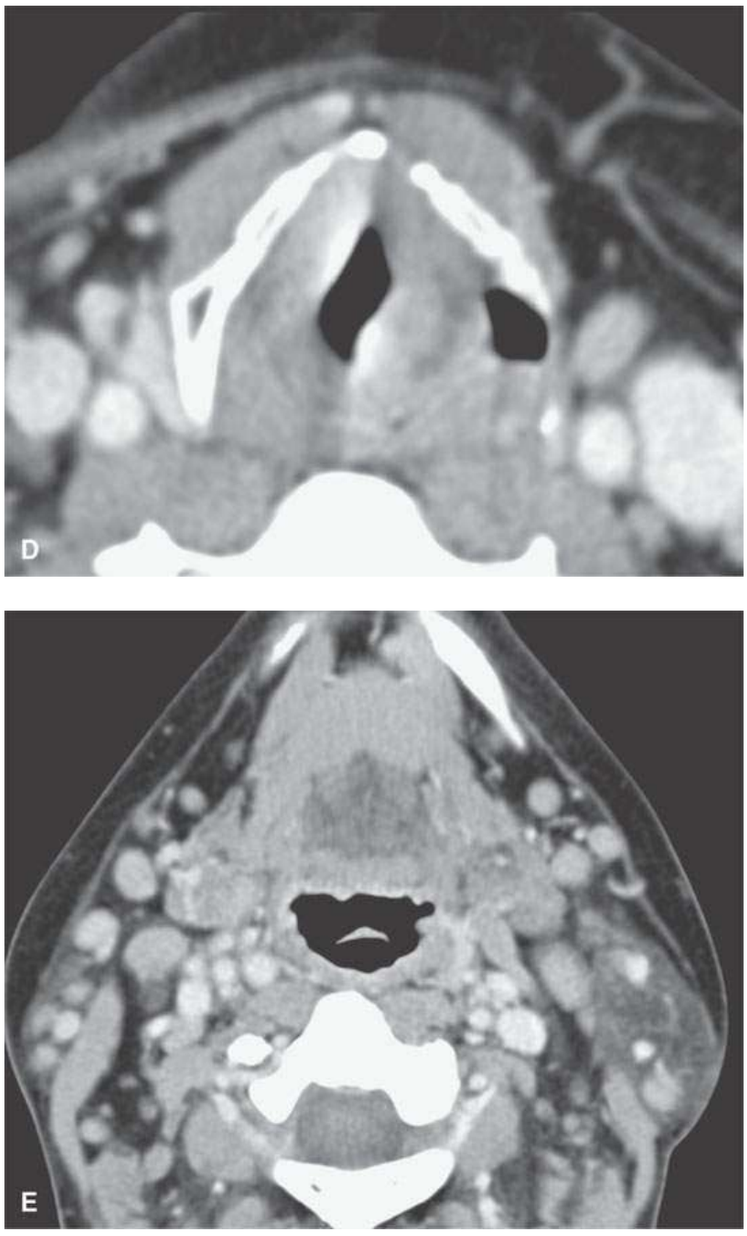

FIGURE 27.12. Contrast-enhanced computed tomography studies of two patients with laryngeal lymphoma**. A**, **B:** In the first patient, the lymphoma is confined to the glottic and subglottic levels and is indistinguishable from squamous cell carcinoma**. C–E:** The second patient had predominantly supraglottic disease with involvement of the false cord and aryepiglottic fold with generalized cervical adenopathy **(E).**

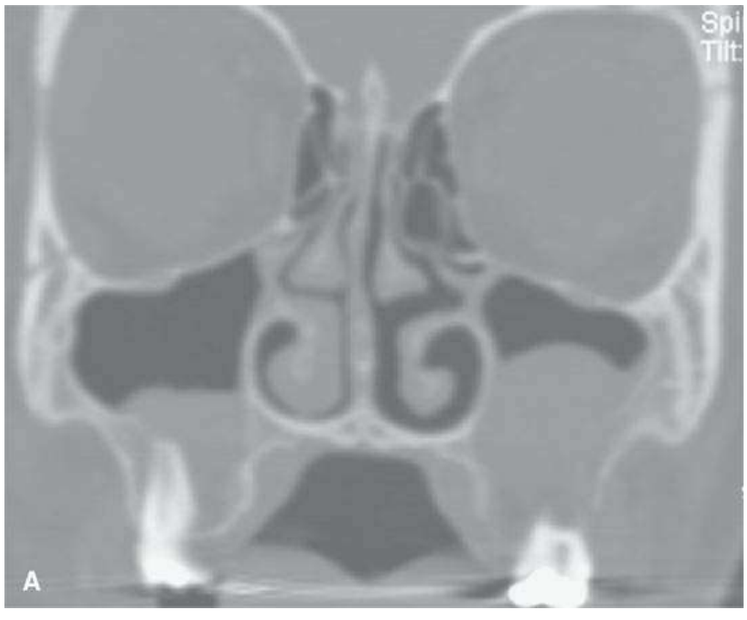

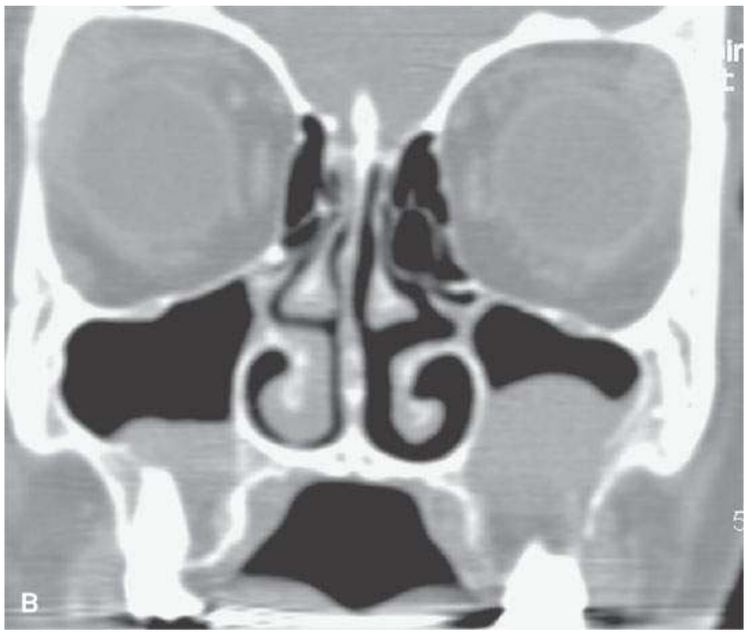
B

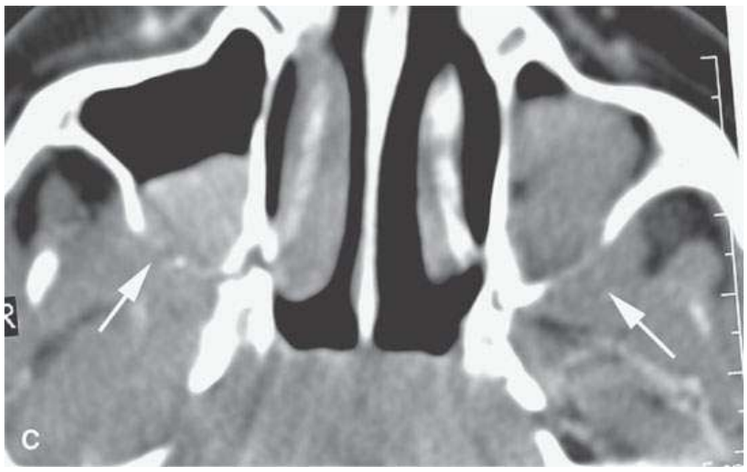
R
C

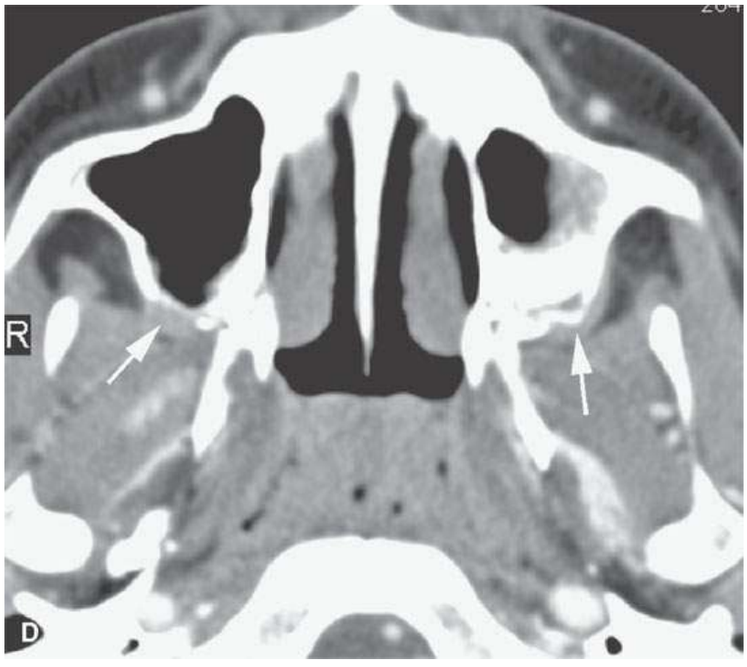
R
D

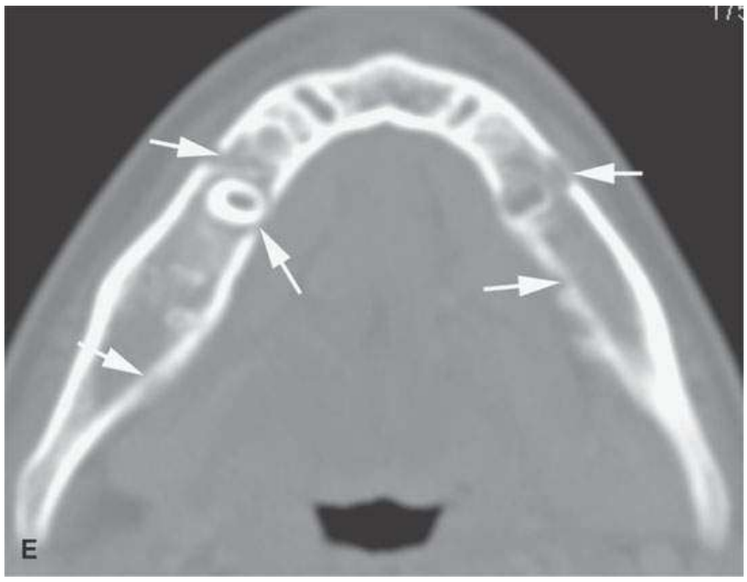
E

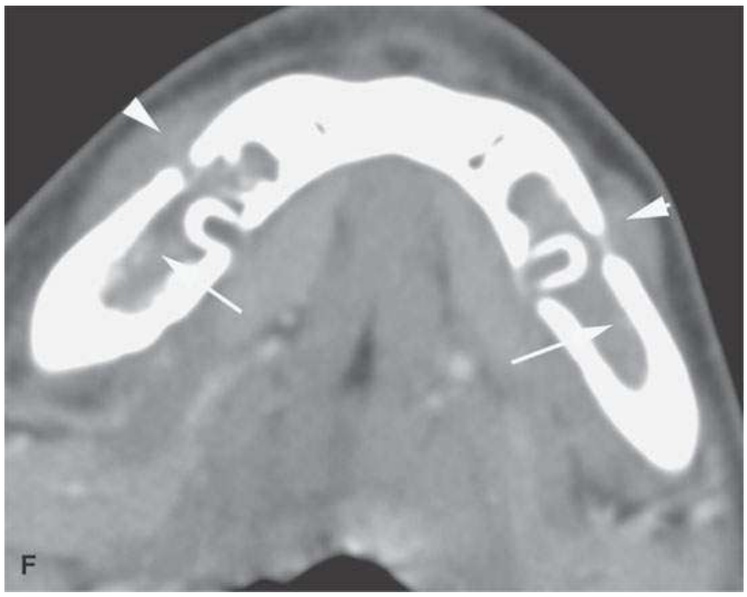
F

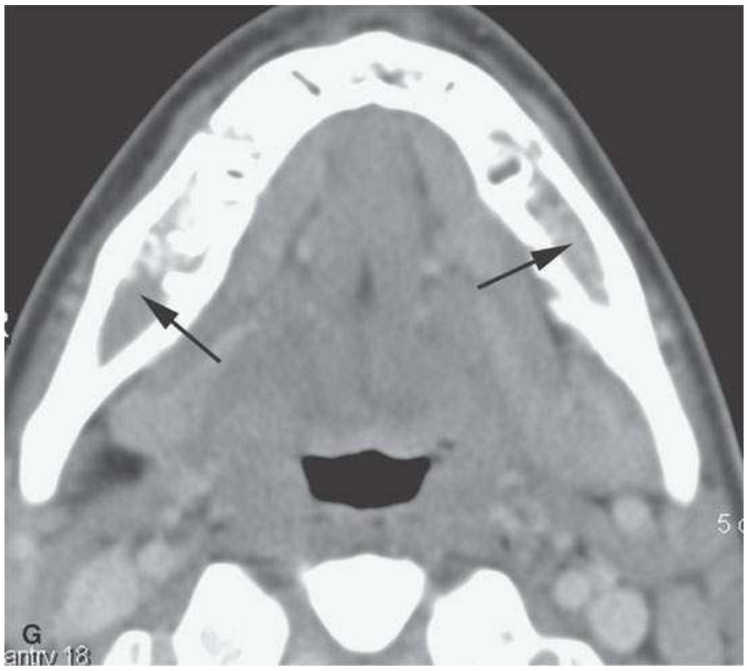
G

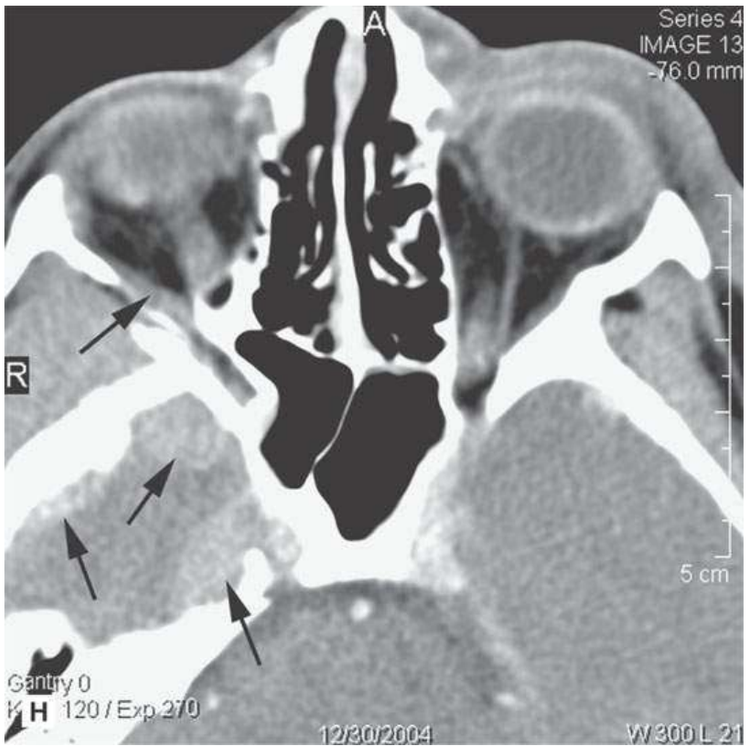

FIGURE 27.13. A 15-year-old male presenting with facial pain and loose teeth proven to be due to Burkitt lymphoma**. A–D**: Contrast-enhanced computed tomography showing masses involving both upper gingivobuccal sulci and maxillary sinuses with infiltration of the retroantral fat (*arrows* in **C** and **D**)**. E:** Erosion of the lingual and buccal surfaces of the mandible *(arrows)***. F**, G:Soft tissue spread *(arrowheads)* via the mental foramina with tumor filling the mandibular marrow space *(arrows)* with continued filling of the marrow space (*black arrows* in **G**)**. H:** Skull base, orbital, and dural invasion were present as well *(arrows)***.**

A particular spread pattern of some B-cell lymphomas that is recognized more frequently now with modern imaging is lymphoma that spreads along nerves and vessels.5 Angiotropic spread patterns can be seen in some types of B-cell lymphoma**.** This angiotropic spread pattern is within and around vessels, but it is not innately destructive of the vessel; thus, it does not result in tissue necrosis**.** Angiotropic spread can be seen along the intracranial and extracranial course of the vessels. It is most commonly visible extracranially along the distal maxillary artery pedicle in the pterygopalatine fossa and its more distal branches within the fat pad posterior to the maxillary sinus (Fig. 27.2)**.** Angiocentric growth involves the vessel much as a vasculitis, and its growth in and along vessels is associated with adjacent tissue necrosis (Fig. 27.14)**.** The angiocentric B-cell lymphomas are Epstein-Barr virus associated and in the head and neck are most often manifest in the brain**.**6

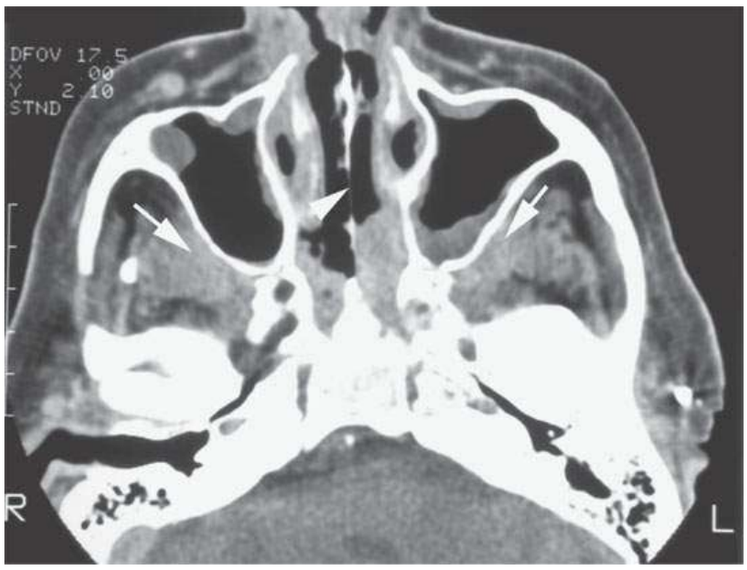

FIGURE 27.14. Contrast-enhanced computed tomography of a patient with angiocentric lymphoma with necrosis of the nasal septum *(arrowhead)* and other nasal cavity infiltrating disease and invasion of the infratemporal fossa bilaterally *(arrows)***.**

Perineural spread can be seen along the intracranial and extracranial course of the cranial nerves and/or associated vascular structures (Figs. 27.15 and 27.16)**.** This perineural spreading of lymphoma must be differentiated from perineural spread of skin cancers as well as adenoidcystic and other glandular neoplasms**.**

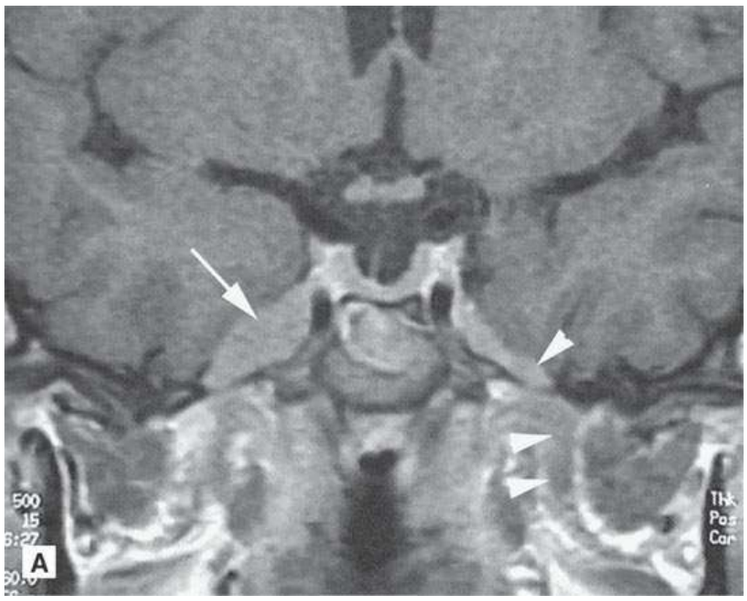
A

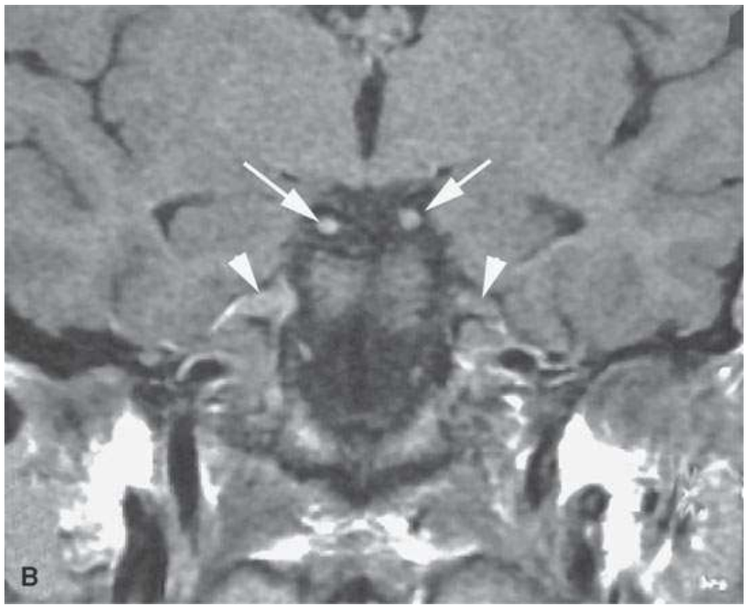
B

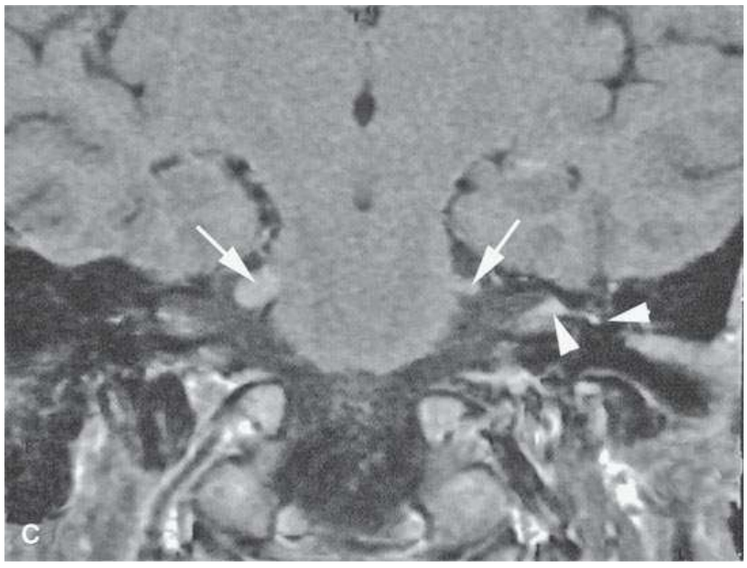
C

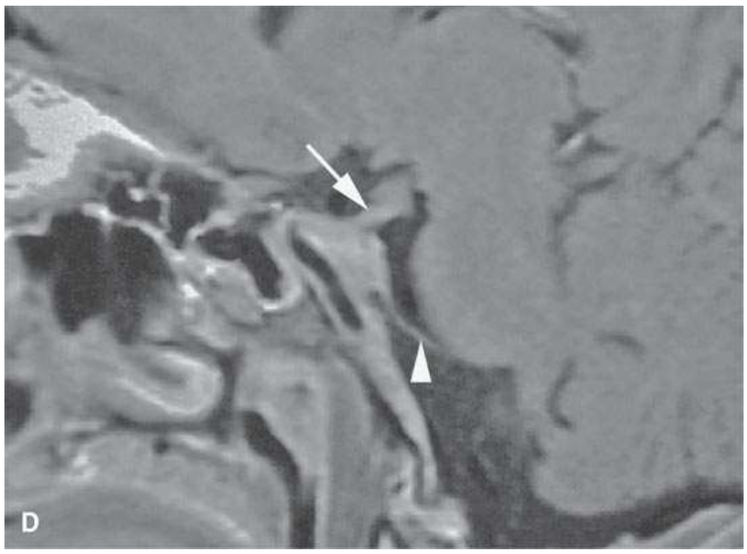
D

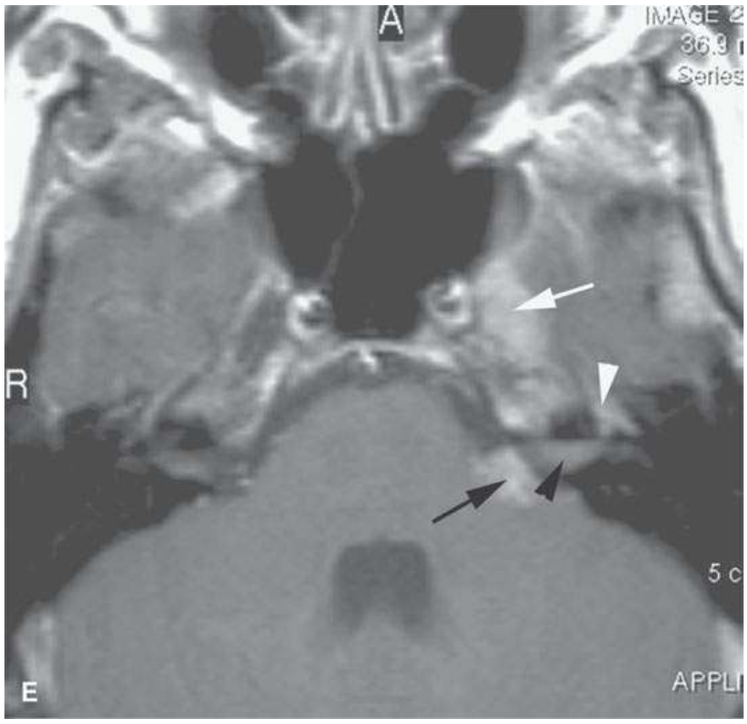
A
R
E

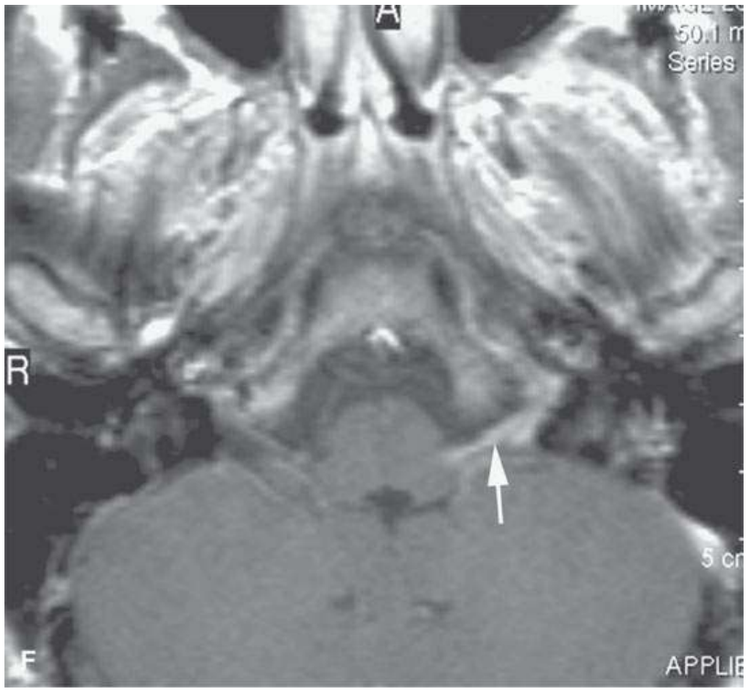
A
R
F

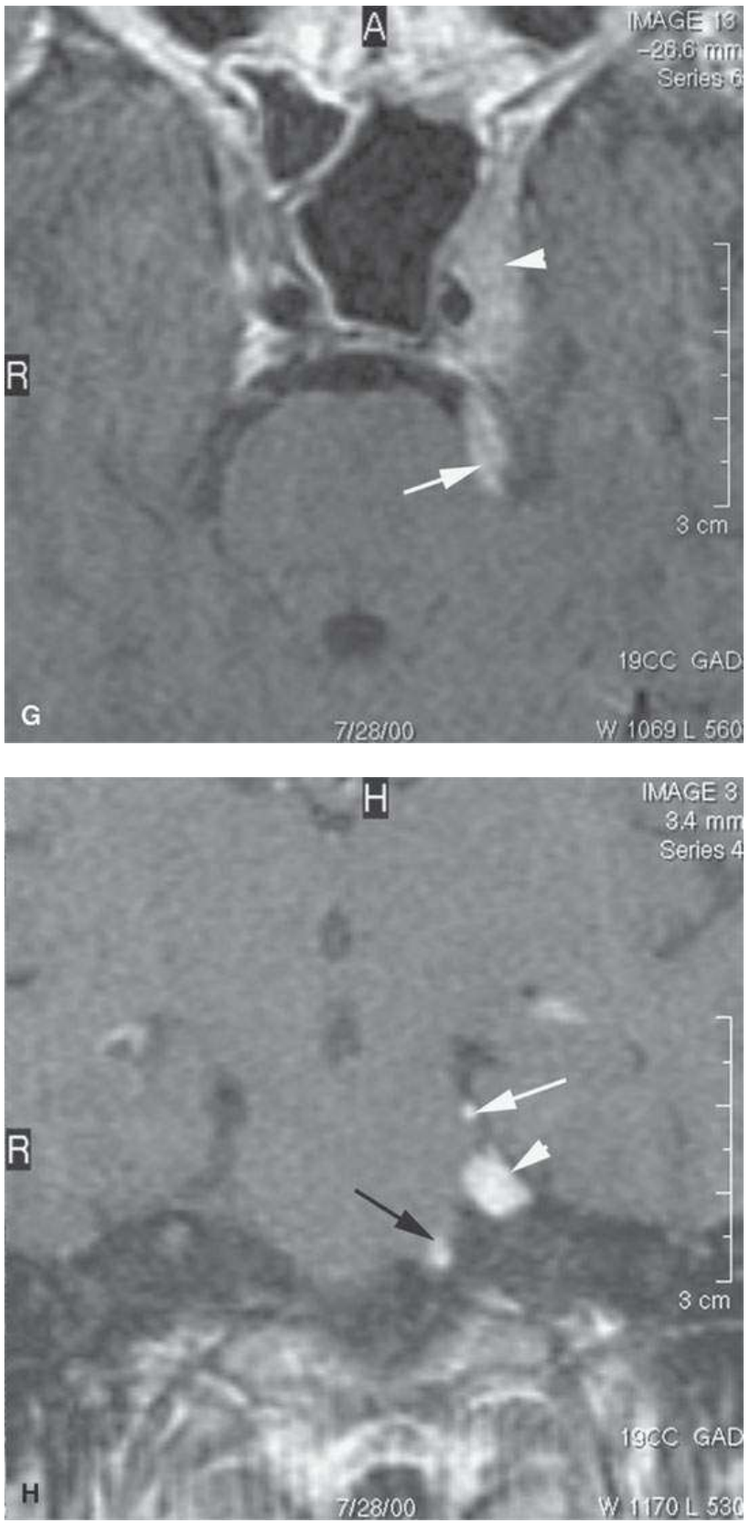

FIGURE 27.15. Two patients with neurotropic lymphoma. Contrast-enhanced magnetic resonancestudy of a patient with neurotropic lymphoma conforming to the nerve anatomy manifest by enlargement and minimal enhancement of the affected nerves. **A**: The trigeminal nerves *(arrows)* and ganglia *(arrowhead)* are involved bilaterally. **B**: The third cranial nerves *(arrows)* and trigeminal nerves *(arrowheads)* are involved bilaterally. **C**: The trigeminal nerves are affected at their root entry zone *(arrows)*, and there is involvement of the facial and eighth cranial nerve on the left *(arrowheads)*. **D**: Involvement of the sixth *(arrowhead)* and third cranial nerves *(arrow)*. A second patient with neurotropic lymphoma manifest by infiltration around the nerves by more obviously enhancing tissue than is seen with the patient in **(A) through (D). E**: The trigeminal cistern *(white arrow)*, cerebellopontine angle cistern *(black arrow)*, internal auditory canal *(arrowhead)*, and first genus of the facial nerve *(white arrowhead)* are involved. **F**: The medullary cistern course of the cranial nerves of the jugular fossa (IX–XI) is involved *(arrow)*. **G**: The cisternal involvement of the fifth cranial nerve follows the nerve to its root entry zone. **H**: The cisternal segment of the fourth *(white arrow)*, fifth *(arrowhead)*, and sixth *(black arrow)* cranial nerves are enlarged and enhance abnormally.

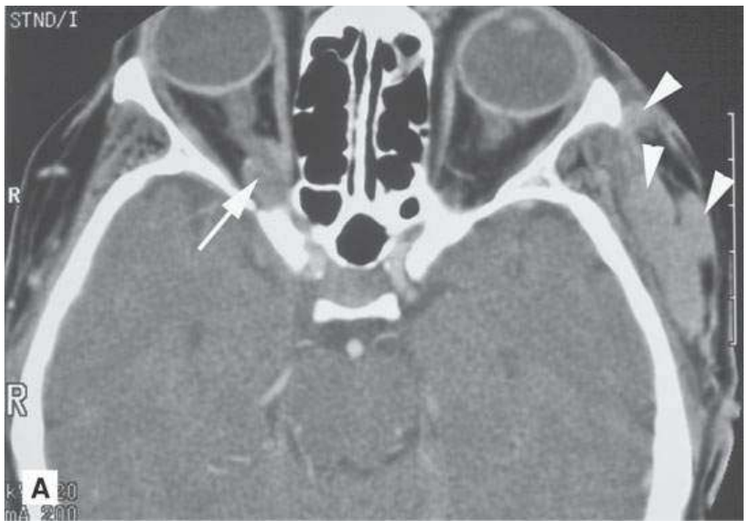
STND/I
R
R
A

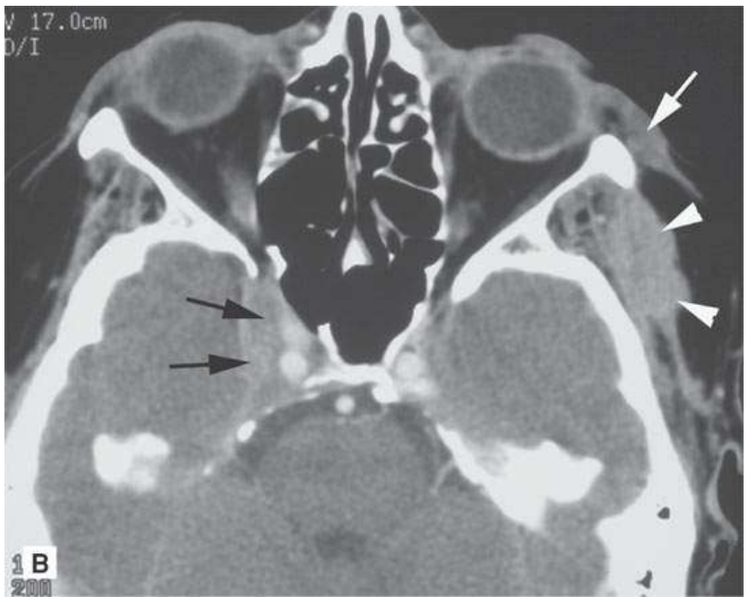
17.0cm
D/I
B

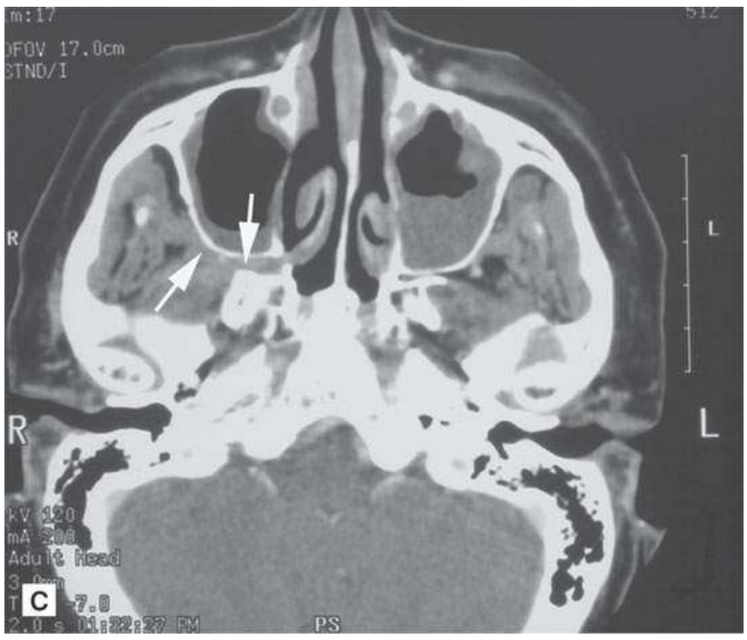
FOV 17.0cm
STND/I
R
L
R
L
kV 120
Adult Head
C
PS

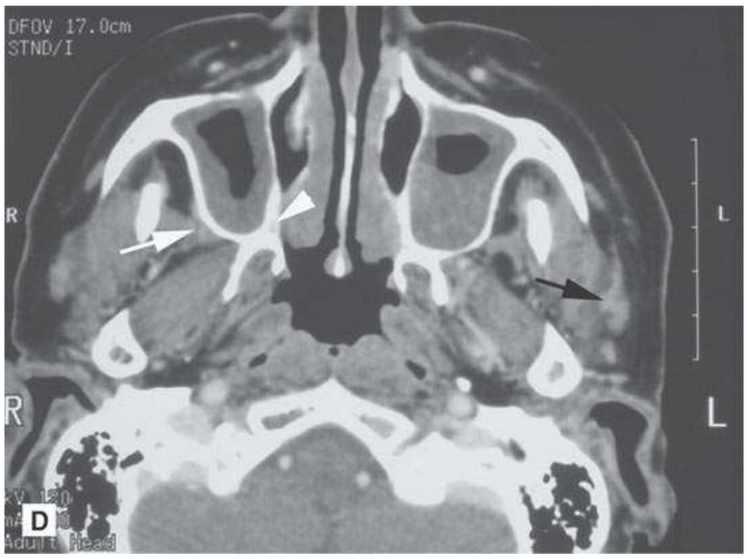
DFOV 17.0cm
STND/I
R
L
R
L
D

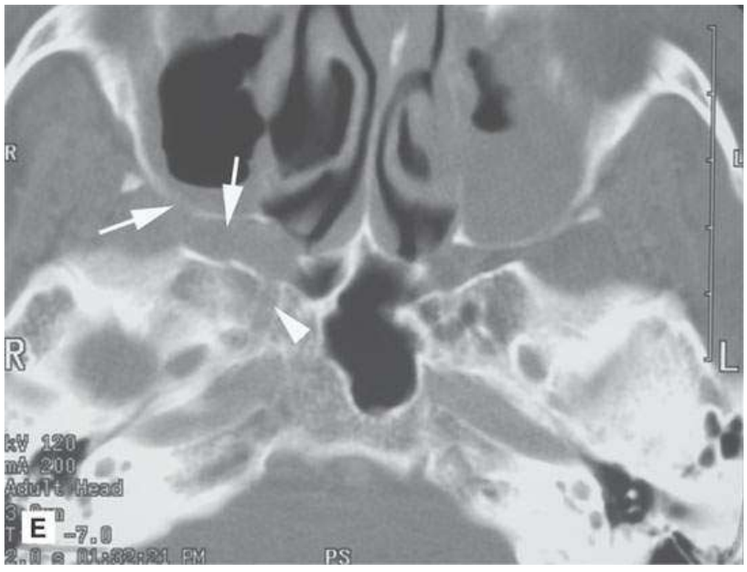
R
L
R
L
kV 120
mA 200
Adult Head
E
-7.0
PS

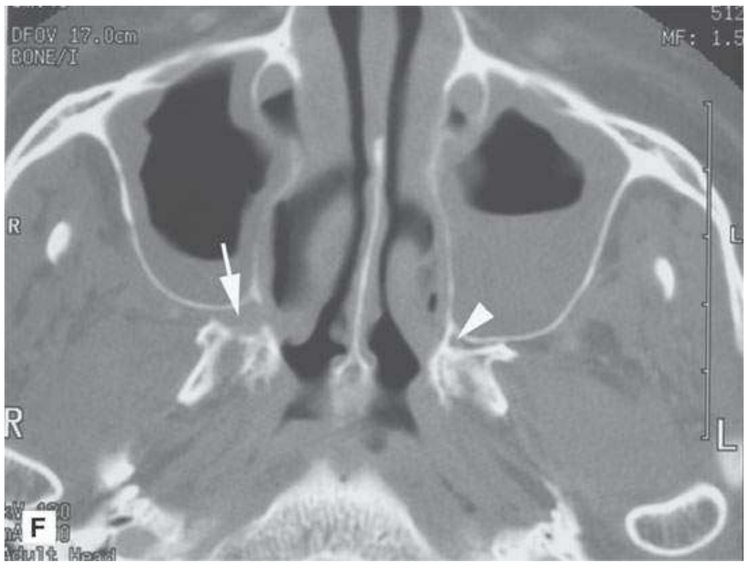
DFOV 17.0cm
BONE/I
MF: 1.5
R
L
R
L
F

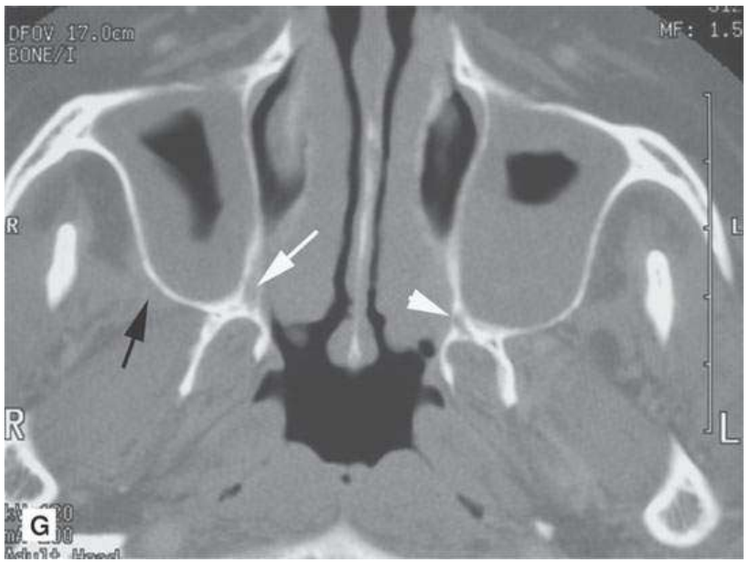

FIGURE 27.16. Contrast-enhanced computed tomography study of a patient with neurotropic lymphoma conforming to the nerve anatomy manifest by enlargement and minimal enhancement along the course of the affected nerves and obliteration of tissue planes around those nerves with remodeling of adjacent bones. **A**: Spread along the cranial nerves of the cavernous sinus into the orbit via the superior orbital fissure *(white arrow)*. Thickening along the zygomatic division branches of the facial nerve *(arrowheads)*. B: Spread along the cranial nerves of the cavernous sinus *(black arrows)*. Thickening along the zygomatic division branches of the facial nerve (*white arrows* and *arrowheads*). **C**: Spread along the posterior superior alveolar branches of V2 *(arrows)* with enlargement of the pterygopalatine fossa *(arrows)*. **D**: Spread along the posterior superior alveolar branches of V2 *(arrows)* and enlargement of the greater palatine foramen due to involvement of that branch of V2 *(arrowheads)*. Thickening of the zygomatic division of the facial nerve *(black arrow)*. **E**: Bone windows showing enlargement of the pterygopalatine fossa *(arrow)* and vidian canal *(arrowhead)*. **F**: Bone windows showing enlargement of the pterygopalatine fossa *(arrow)* compared to the normal side *(arrow)*. **G**: Bone windows showing enlargement of the greater palatine foramen *(white arrow)* compared to the normal side *(arrowhead)* and no bone erosion where the posterior superior alveolar nerve is involved *(black arrow)*.

Extranodal Trends in T-Cell Lymphomas

The T-cell lymphomas are generally nodal malignancies; when there is extranodal disease, it is typically of the Waldeyer ring.7 Mycosis fungoides is an exception that will present at virtually any mucosal site or the skin as localized papules that may be necrotic due to the associated vasculitis as well as in nodes. Other T-cell lymphomas may involve the skin. Some can present as necrotizing retinal lesions.

The angiocentric T-cell lymphomas predominantly involve the nasal cavity and the sinus and nodes8(Fig. 27.14).8 These used to be called by a variety of names, including *Lethal lethal Midline midline Granulomagranuloma*; *polymorphic reticuloses*; and, in the lung, *lymphomatoid granulomatosis*. Those terms have been discarded.

Hodgkin Disease

Hodgkin disease most commonly presents as a neck node. The disease may grow out of any node to invade local soft tissues, but de novo soft tissue disease does not occur. Clinical extranodal disease is uncommon, but occult involvement of the Waldeyer ring may be present in as many as 15% to 20% of patients.9 This is likely related to this disease spreading contiguously within the lymphatic system to both nodes and organs that contain lymphoid tissue. Extranodal disease may also involve the sinonasal region but in general clinical and imaging evidence of extranodal disease in the head and neck is very unusual at presentation. It may be more common in relapsed disease.

GENERAL INDICATIONS FOR IMAGING

Imaging is useful in staging, follow-up, and occasionally planning adjunctive surgery. The relative roles of computed tomography (CT) and radionuclide studies such as gallium and fluorine-18 2-fluoro-2-deoxy-D-glucose positron emission tomography (FDG-PET) are constantly being redefined. Currently, a mix of anatomic and physiologic imaging is used in no universally agreed upon manner. Magnetic resonance imaging (MRI) is only a primary choice for these purposes when there is known or suspected intracranial disease and especially when the disease demonstrates a tendency for spread along nerves or vessels.10

IMAGING APPEARANCE

General Appearance

Normal or hyperplastic (Fig. 26.4) and lymphoma-involved (Fig. 27.17) extranodal lymphoid tissue and lymph nodes are essentially tightly packed aggregates of cells with relatively little stroma. As such, they are about isointense to muscle and hypointense to fat on non–contrast-enhanced T1-weighted MRI and slightly hyperintense to fat on T2-weighted MRI.11 On non–contrast-enhanced CT, they are isodense to muscle. On both studies, contrast enhancement is minimal to moderate and homogeneous. The amount of enhancement is not of any predictive value.

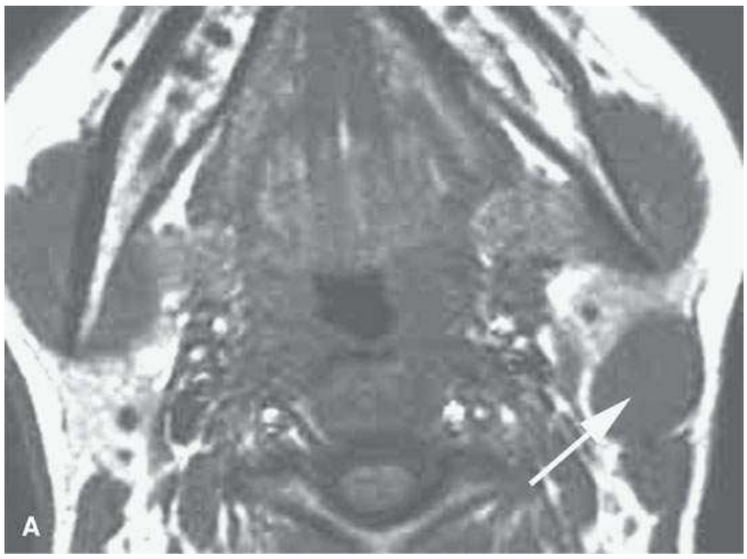
A

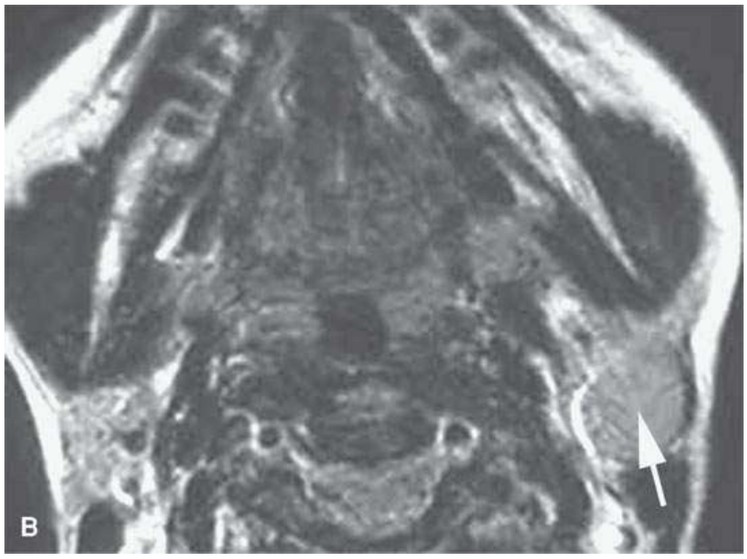
B

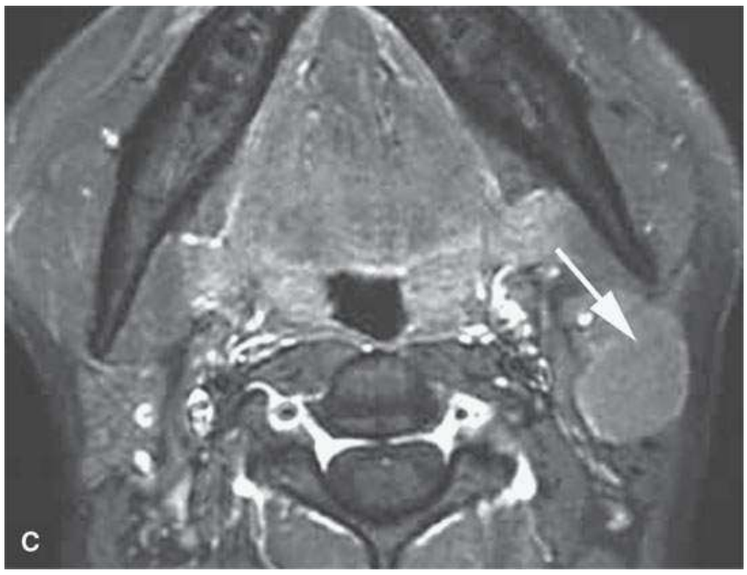
C

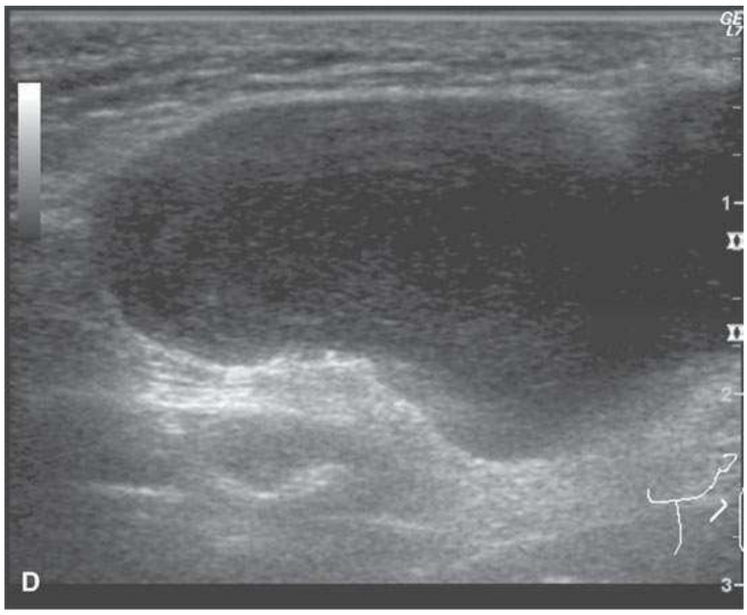

FIGURE 27.17. Lymphomatous node *(arrow)* as seen on magnetic resonance imaging and ultrasound. **A:** T1-weighted (T1W) non–contrast-enhanced image. **B:** T2-weighted image. **C:** Contrast-enhanced T1W fat-suppressed image. **D:** Ultrasound.

Prominent nodal vascular pedicles are seen in larger more reactive nodes on MRI, CT, and ultrasound (Figs. 26.4 and 27.17–27.20). With ultrasound, the resistance index tends to remain relatively low in reactive nodes seen, and flow patterns remain predominantly hilar.[12,13] The resistive index will tend to rise and patterns of enhancement change over to more peripheral in lymphoma-involved nodes, although these findings are not specific and not reliable to supplant biopsy confirmation of disease.

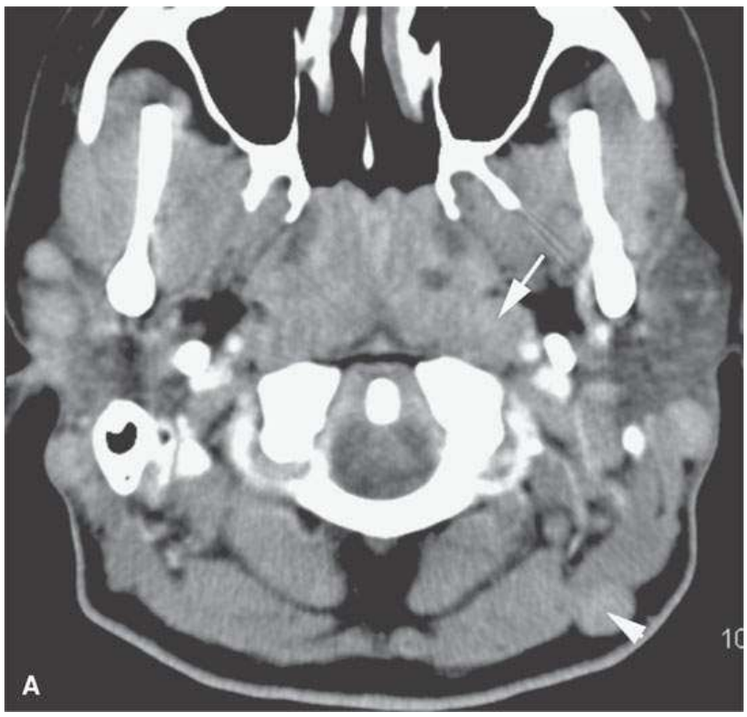

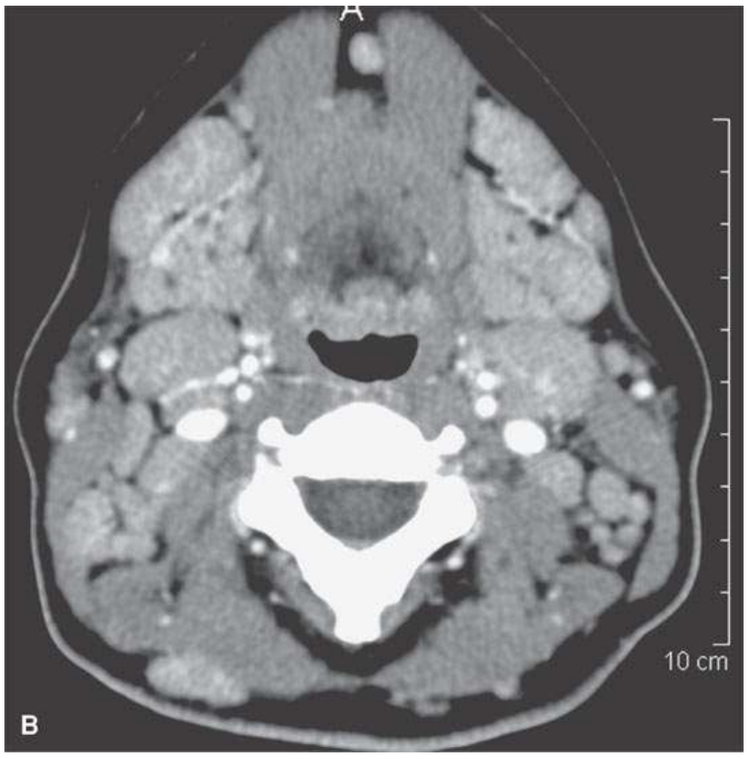
A
10 cm
B

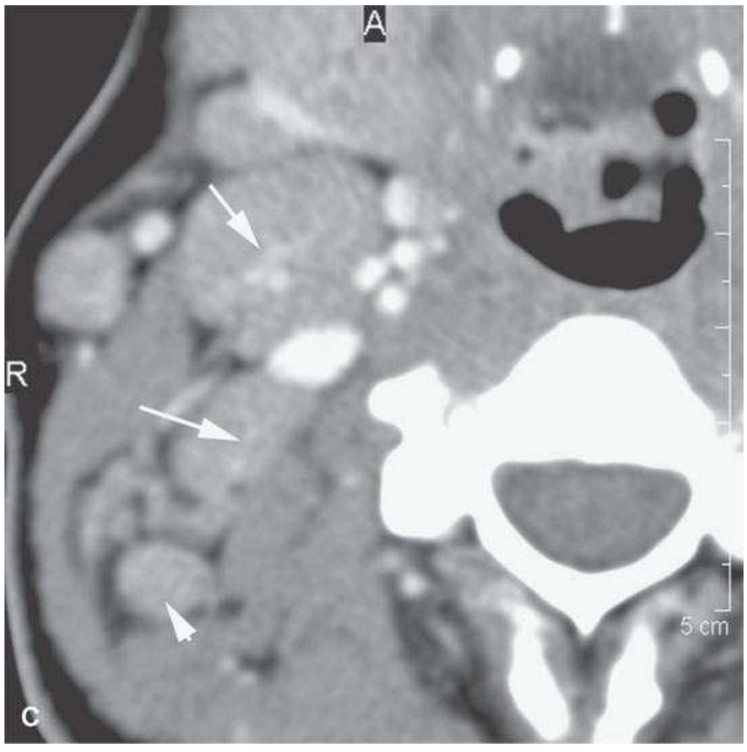
A
R
5 cm
C

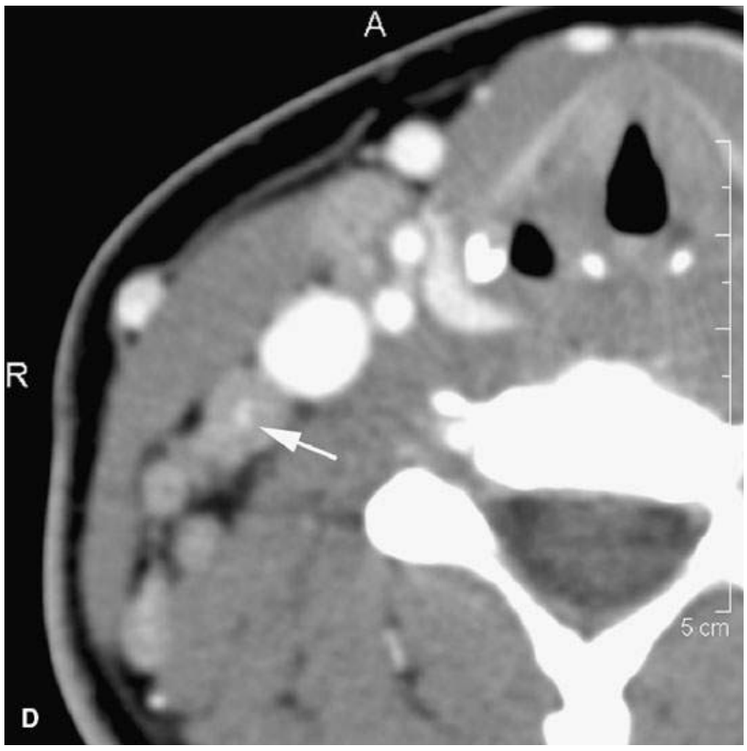
A
R
5 cm
D

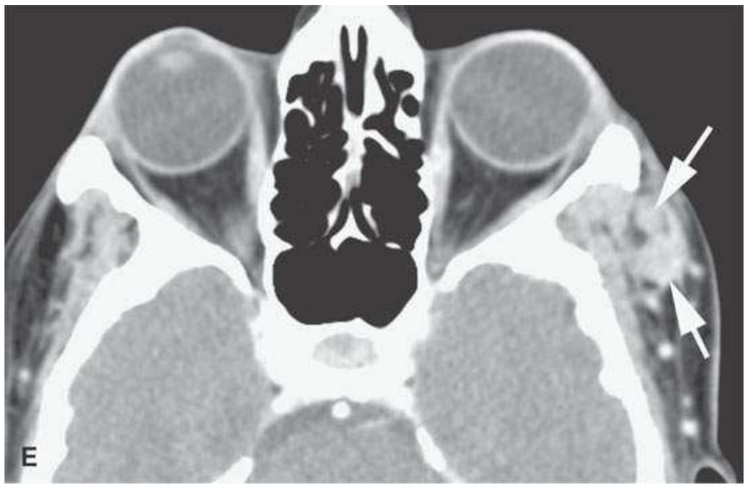
E

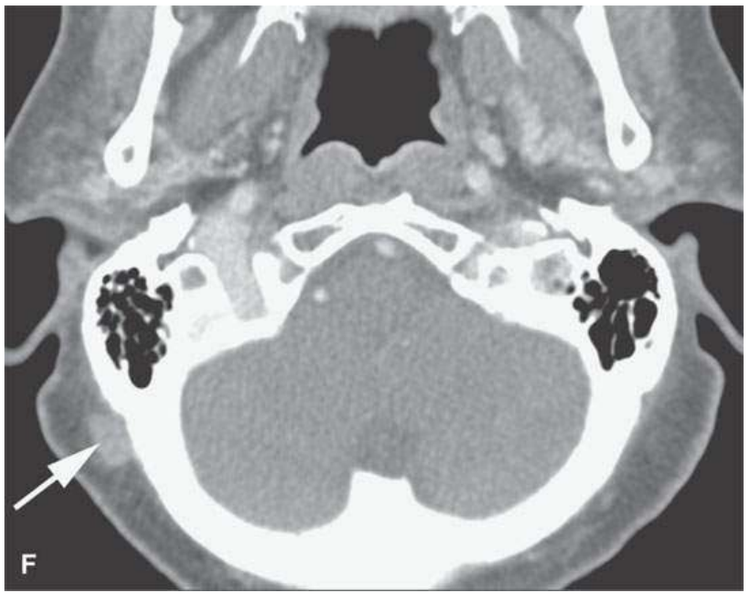
F

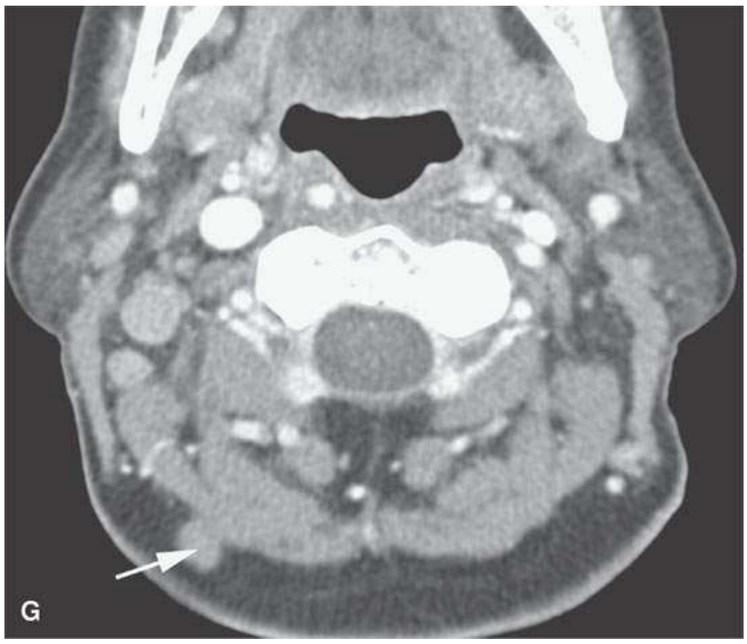

FIGURE 27.18. Lymphomatous node as seen on contrast-enhanced computed tomography. **A:** Parotid, retropharyngeal *(arrow)*, and posterior neck node *(arrowhead)*. **B:** Lymphomatous nodes in all visible groups. **C:** Typical homogenous appearance of lymphomatous node with vascular hilum *(arrows)* visible in larger nodes but not always seen in smaller ones *(arrow)*. **D:** Vascular hilum *(arrow)* visible in a smaller node. **E:** Involved zygomatic node of the facial group. **F:** Involved retromastoid *(arrow)*. **G:** Involved posterior neck node *(arrow)* of the facial group.

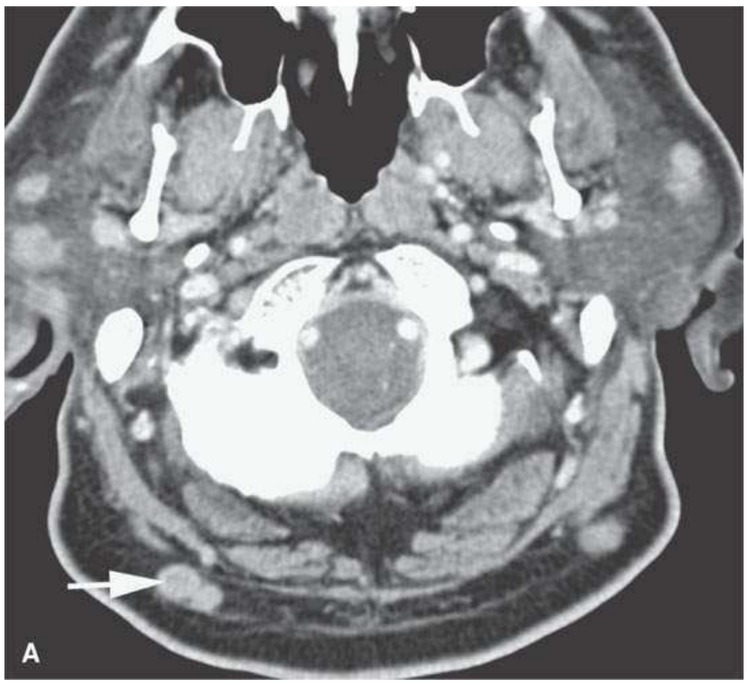

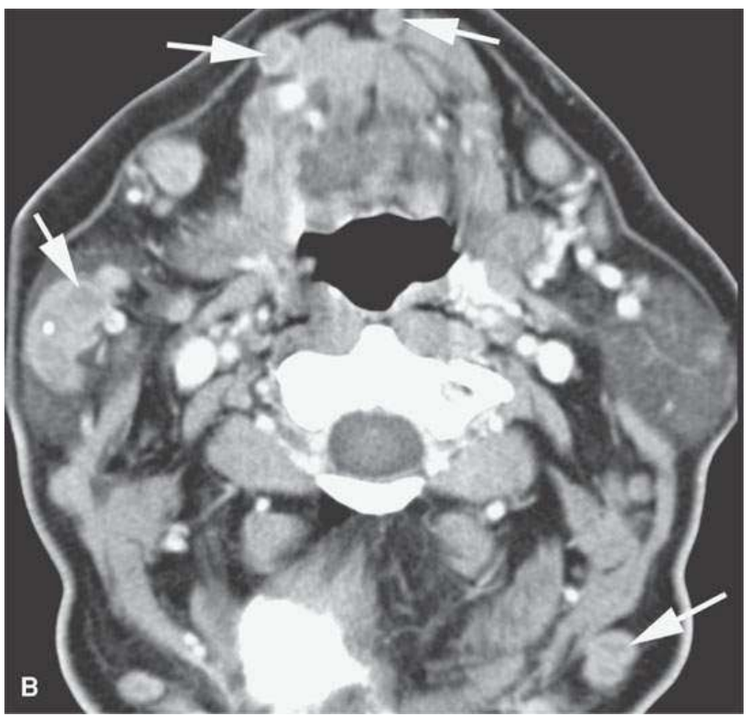

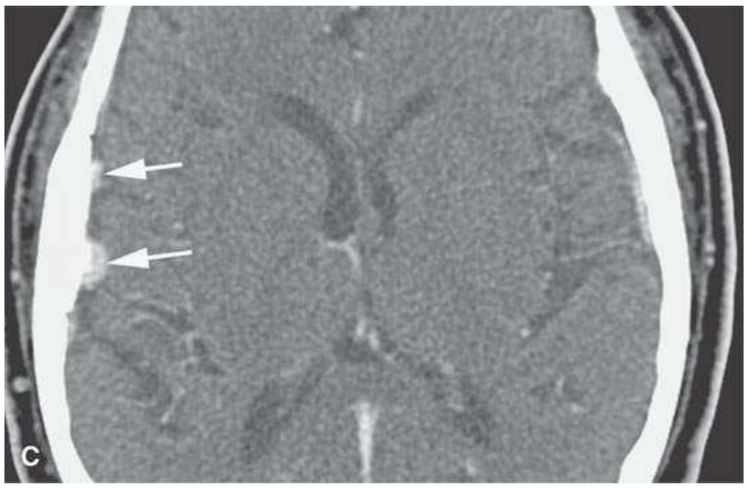

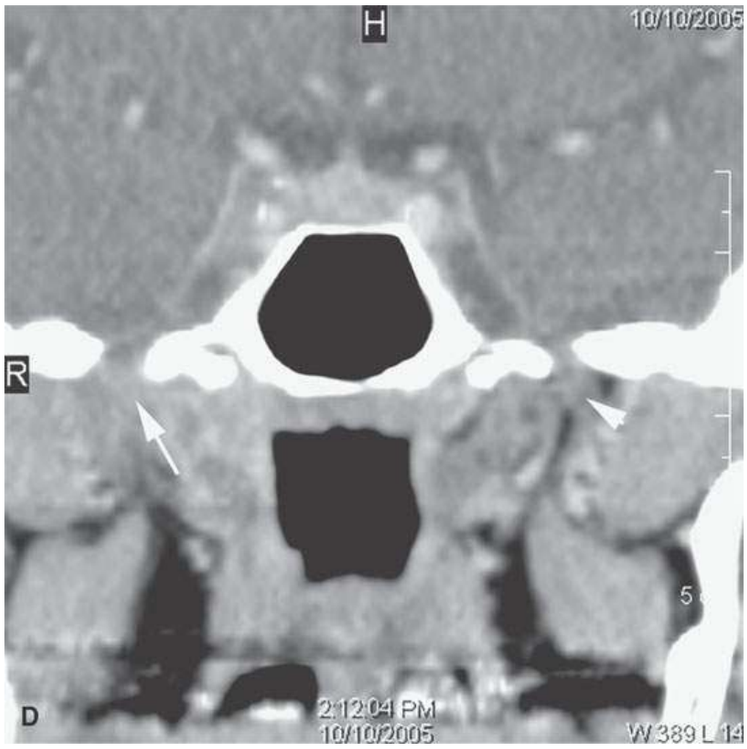

FIGURE 27.19. Contrast-enhanced computed tomography of an aggressive lymphoma**. A, B:** Multiple small positive nodes, many with focal defects due to lymphomatous deposits *(arrows)***. C:** Meningeal lymphomatous involvement *(arrows)***. D:** Perineural involvement of V2 at the foramen ovale *(arrow)***.**

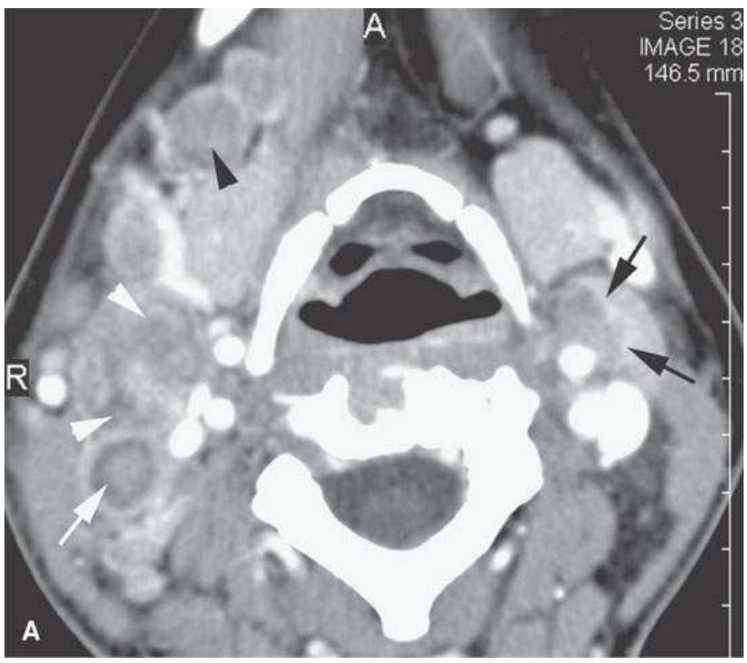

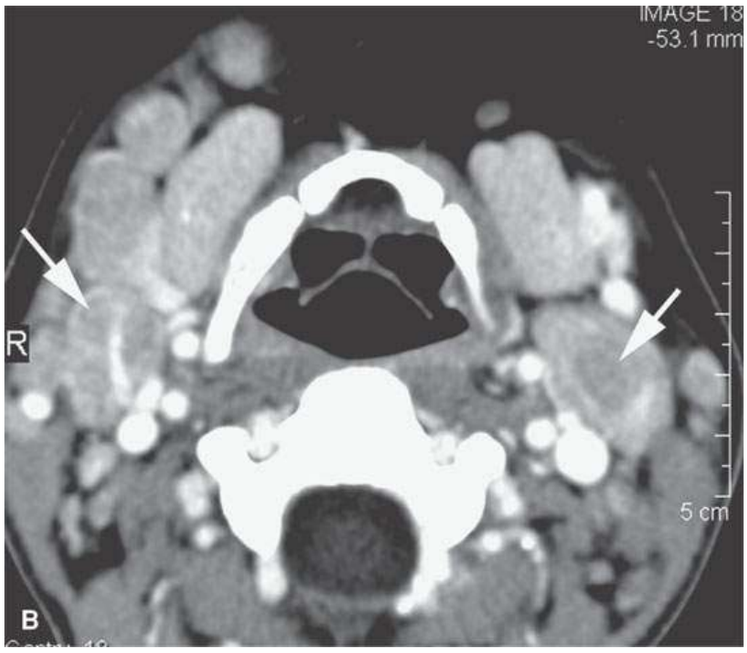
IMAGE 18
-53.1 mm
R
5 cm
B

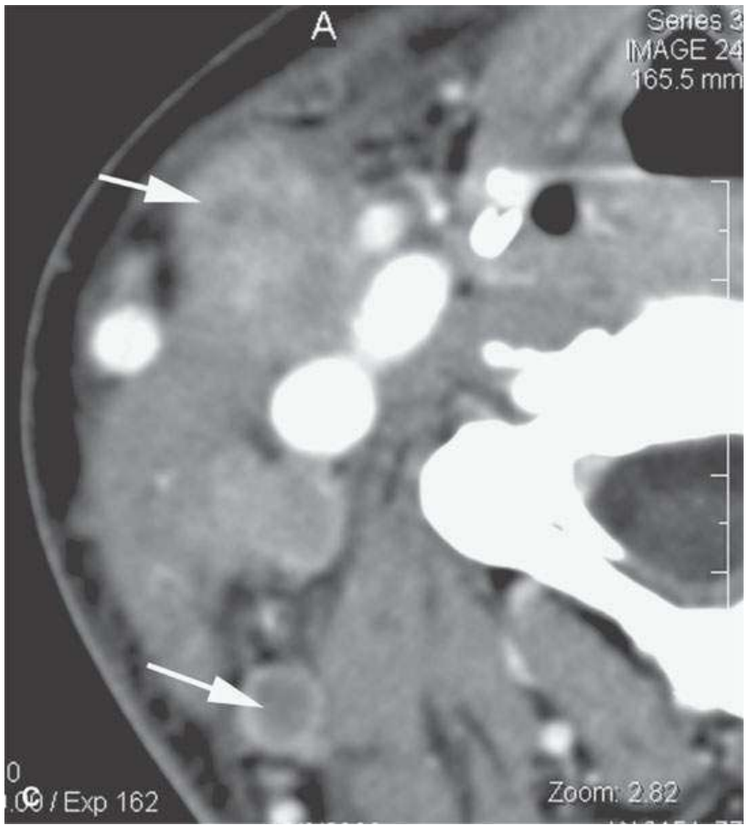
A
Series 3
IMAGE 24
165.5 mm
Zoom: 2.82

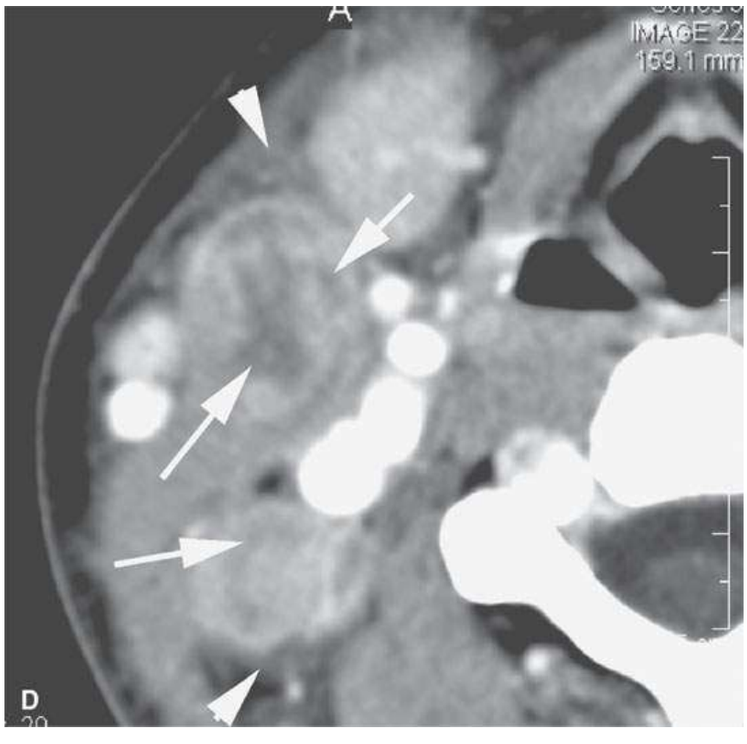
A
IMAGE 22
159.1 mm
D

FIGURE 27.20. Contrast-enhanced computed tomography of unusual variable nodal morphology of lymphoma at the time of original presentation (in an HIV-positive patient) and prior to any treatment **(A, and B)** and nodal necrosis in a treated patient **(C, and D). A:** Eccentric defect in a node *(black arrows)*, complete parenchymal replacement *(black arrowhead)*, irregular replacement in a large node *(white arrowheads)*, targetlike appearance due to peripheral node infiltration *(white arrow)*. **B:** Partial parenchymal replacement by lymphoma in larger nodes *(arrows)*. **C, D:** Areas of probable frank necrosis *(arrows)* and perinodal edema *(arrowheads)*.

Issues related to lymph node morphology in benign and malignant disease are discussed in more detail in Chapters 157 and 158, which are related directly to lymphadenopathies. Lymphoma tends to involve nodal groups that are much less frequently involved in other malignancies, such as the facial and posterior neck nodes.

Necrosis in nodes or soft tissues is seen in lymphoma in response to therapy, in very aggressive disease type, and/or if the patient is HIV positive or otherwise immune compromised (Figs. 27.18–27.20).

Specific Findings

Nodal disease is the most common finding in head and neck lymphoma and is most frequently seen in isolation (Figs. 27.17–27.20). Nodal disease is often present when there is extranodal disease.

Localized infiltrating soft tissue masses are the most common extranodal manifestation. This is often seen in the Waldeyer ring and is common in the orbit and less so in the nasal cavity and sinuses (Figs. 27.1–27.5, 27.8, and 27.9). The parotid glands (Figs. 27.6 and 27.7) and thyroid gland (Fig. 27.10) are less likely to be involved. Unusual sites of presentation include the canine fossa of the cheek, the buccal space (Figs. 27.11 and 27.13), and the infratemporal fossa (Figs. 27.14 and 27.21), likely due to at least some relationship to the facial nodes and related lymphoid elements in these locations presented in Chapter 149. Disease in the larynx and trachea is rare (Figs. 27.12).

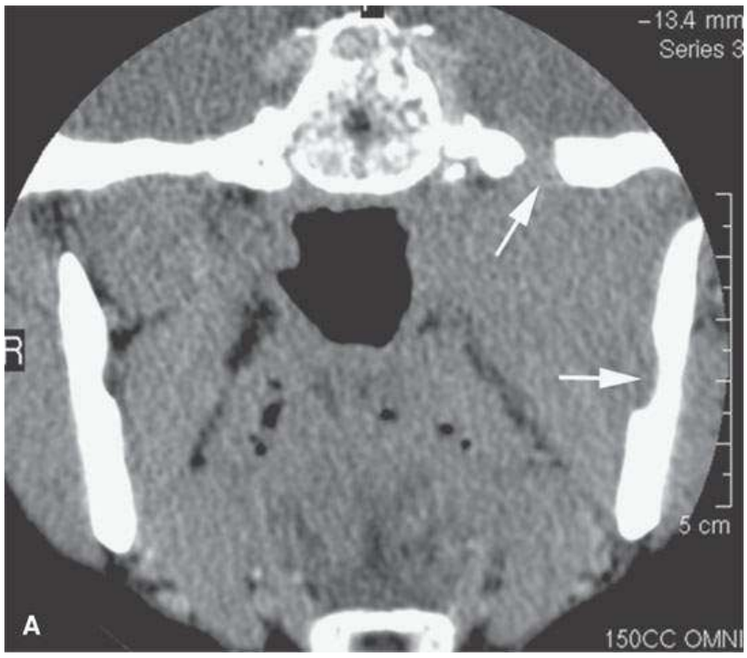

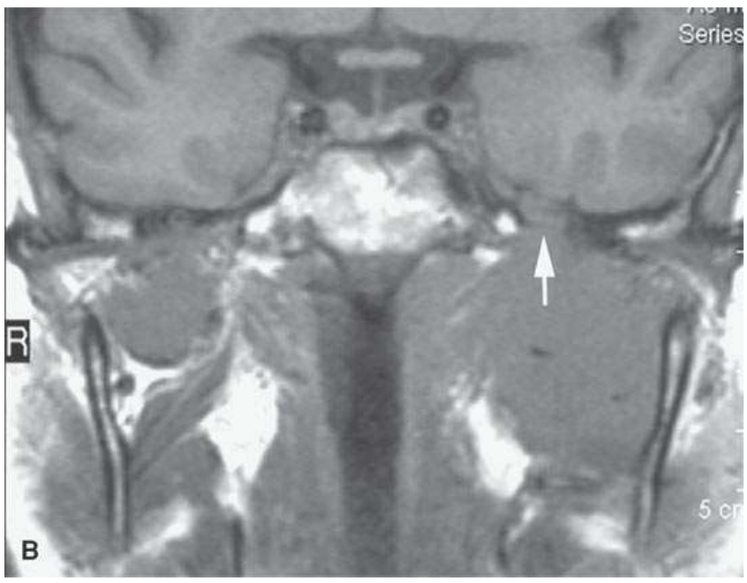

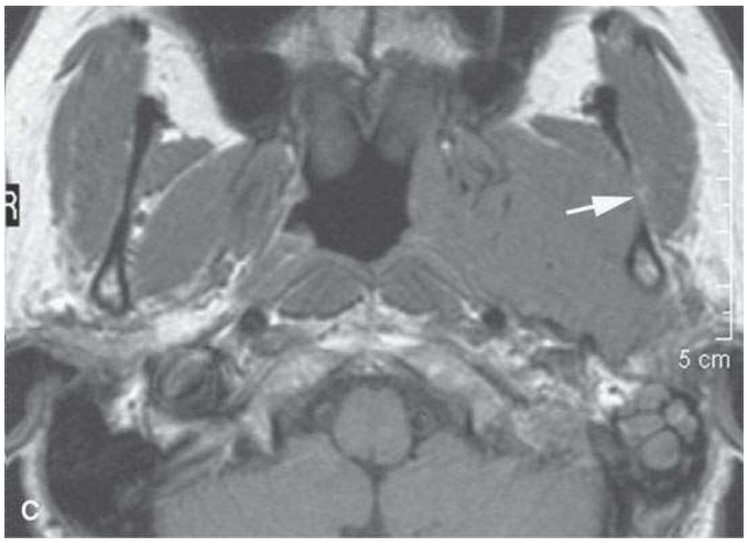
R
5 cm
C

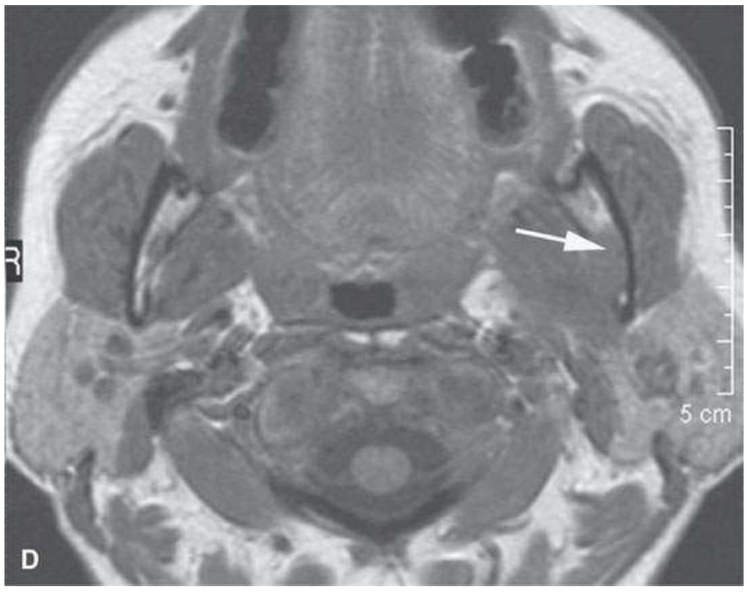
R
5 cm
D

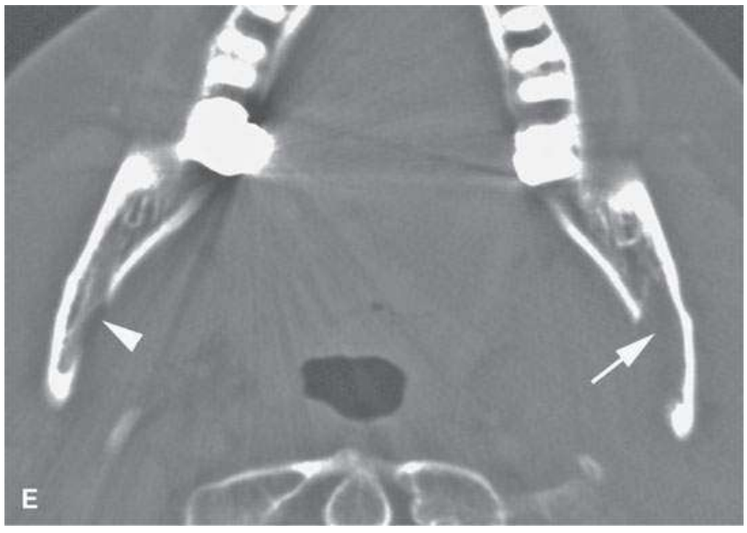
E

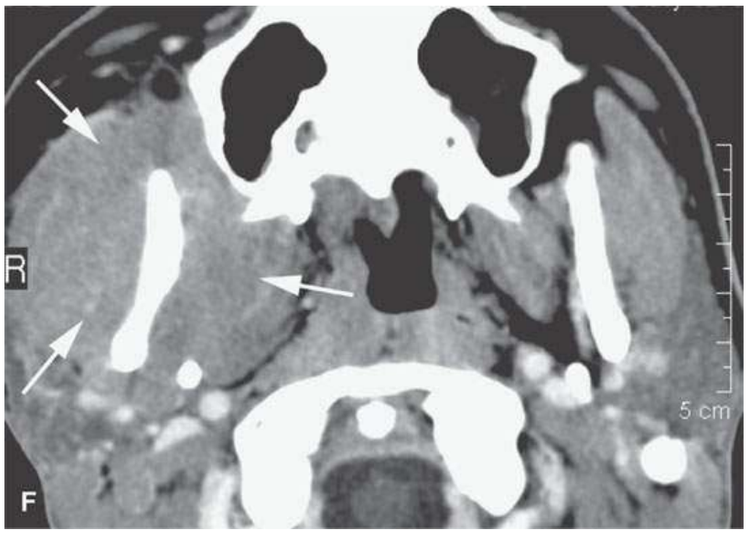
R
5 cm
F

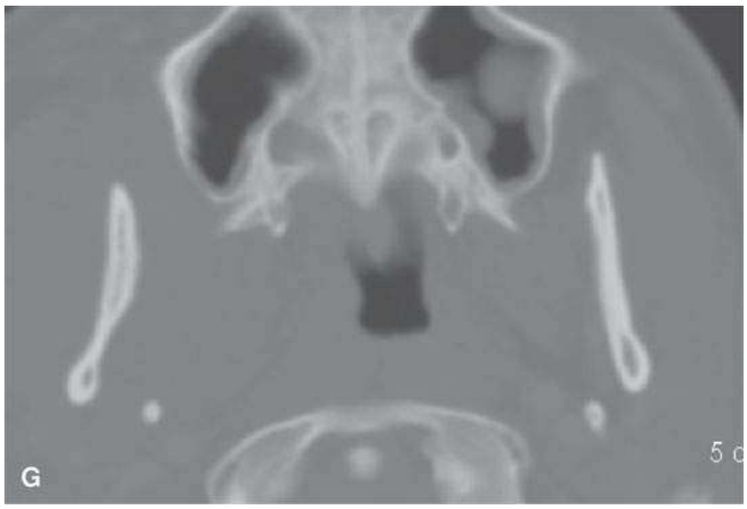

FIGURE 27.21. Computed tomography (CT) and magnetic resonance imaging of two patients with non-Hodgkin lymphoma of the masticator space. **A:** Contrast-enhanced CT of the lymphoma filling the masticator space and spreading to involve V3 at the foramen ovale and inferior alveolar branch of V3 at the mandibular foramen *(arrows)*. **B:** Non–contrast-enhanced T1-weighted (T1W) image correlating with **(A)** *(arrow)* showing foramen ovale involvement. **C:** Non–contrast-enhanced T1W image showing tumor filling the masticator space and eroding the mandible *(arrow)*. **D:** Non–contrast-enhanced T1W image of the lymphoma involving V3 at the mandibular foramen *(arrow)*. **E:** CT at bone windows correlating with **(D)** and showing invasion of inferior alveolar branch of V3 at the mandibular foramen *(arrows)*. **F, G:** Contrast-enhanced CT showing more diffuse masticator space involvement in a second patient by a slightly enhancing (as compared to nonenhancing) lymphoma *(arrows)* with no visible bony mandibular changes.

Perineural and perivascular disease is an uncommon but important mode of spread of lymphoma and may be responsible for its presenting manifestations. Pure perineural disease may be seen intracranially (Fig. 27.15) and sometimes is identifiable as predominantly extracranial spread along nerves (Fig. 27.16). Most cases of extracranial spread could reasonably be considered as a combination of spread along both nerves and vessels that are traveling together, such as the distal maxillary neurovascular bundle and its more distal ramifications. Angiocentric and angiotropic disease can cause cerebral infarcts. Spread along these conduits frequently leads to the cavernous sinus region, where it may first be noticed on imaging examinations.

Bone involvement can be seen as a secondary effect of invasion from a soft tissue site of origin such as the nasopharynx (Figs. 27.1, 27.5, 27.9, 27.11, 27.13, 27.16, and 27.22). Bone destruction due to angiocentric/vasculitic spread pattern is most often seen in angiocentric disease in the sinonasal region. Bone invasion as a primary site of involvement in marrow space disease may manifest as a primarily osteolytic, osteoblastic, or mixed pattern. The bone pattern can overlap with that seen in metastases and skull base osteomyelitis as well as leukemia and plasma cell dyscrasias.

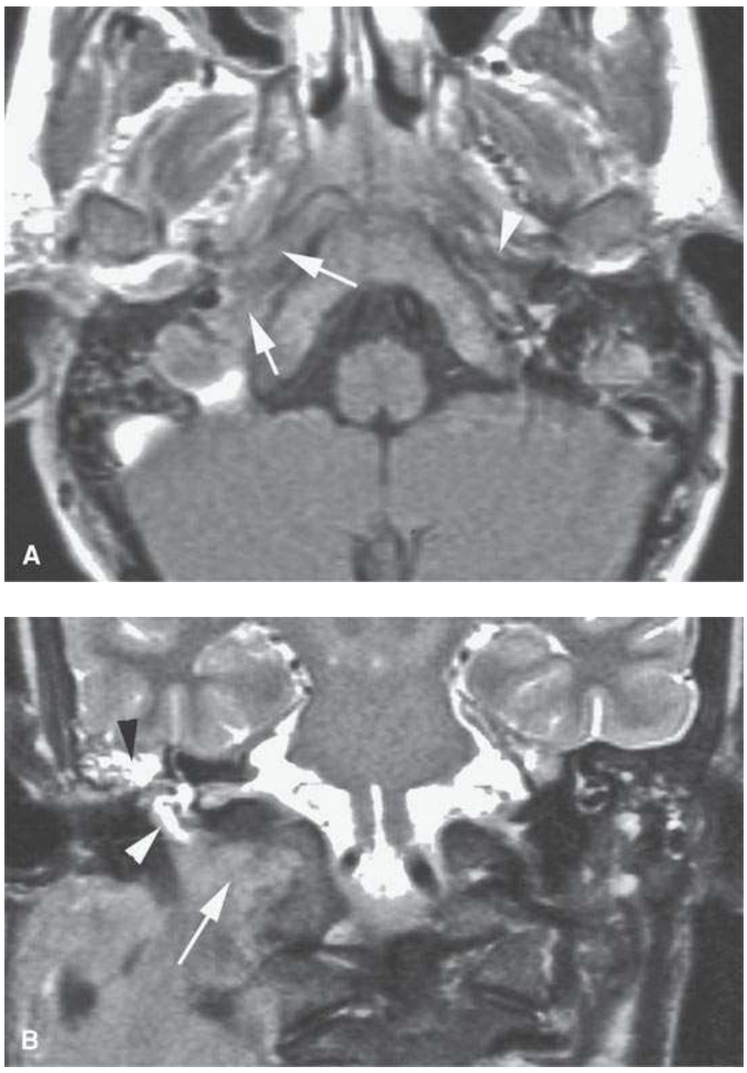

FIGURE 27.22. Magnetic resonance imaging of a patient with non-Hodgkin lymphoma of the petrous apex. **A:** Contrast-enhanced T1-weighted image showing minimally enhancing lymphoma infiltrating the petrous apex and mastoid portions of the temporal bone including the jugular fossa *(arrows)* compared to the normal side *(arrowhead)*. **B:** T2-weighted coronal image showing the lymphoma to be about isointense to gray matter and causing eustachian tube obstruction with tumor extending into the middle ear *(white arrowhead)* and fluid and/or mucosal thickening in the middle ear and mastoid *(black arrowhead)*.

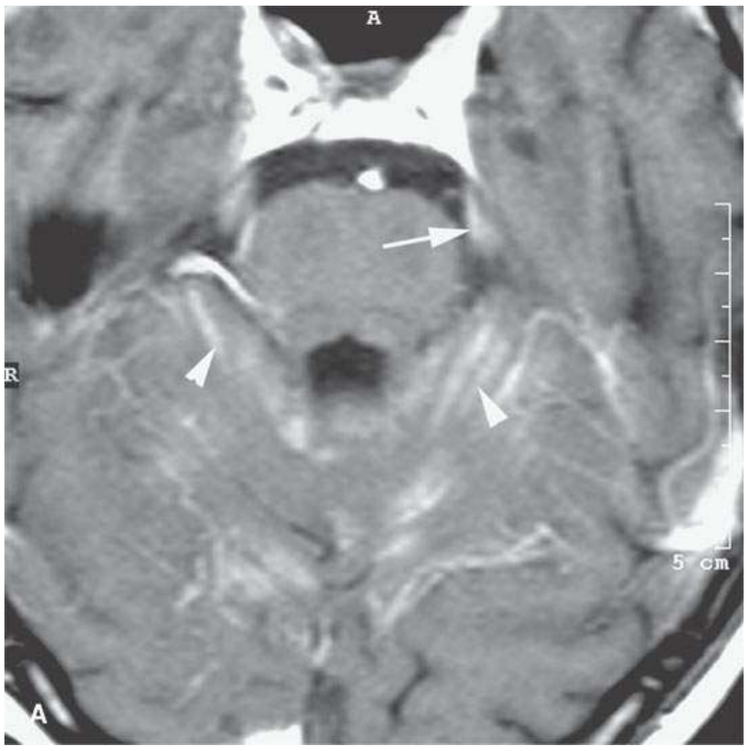
A
R
5 cm
A

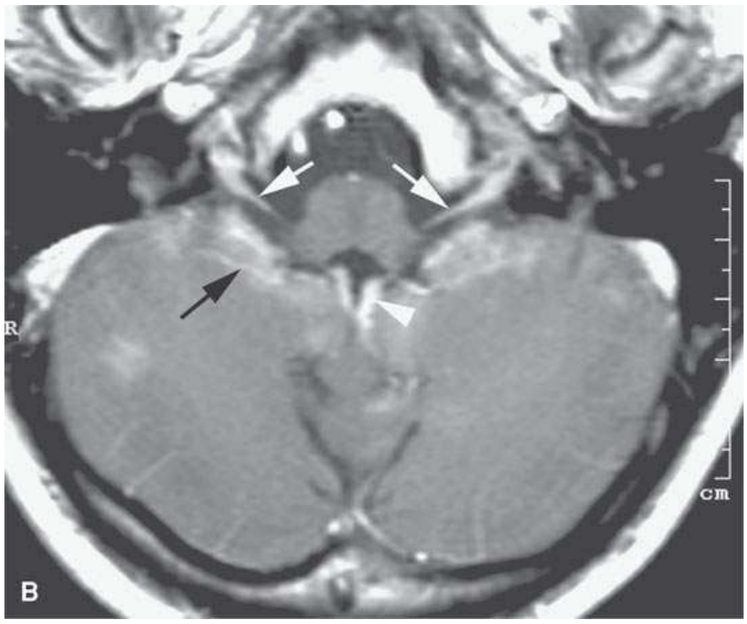
R
cm
B

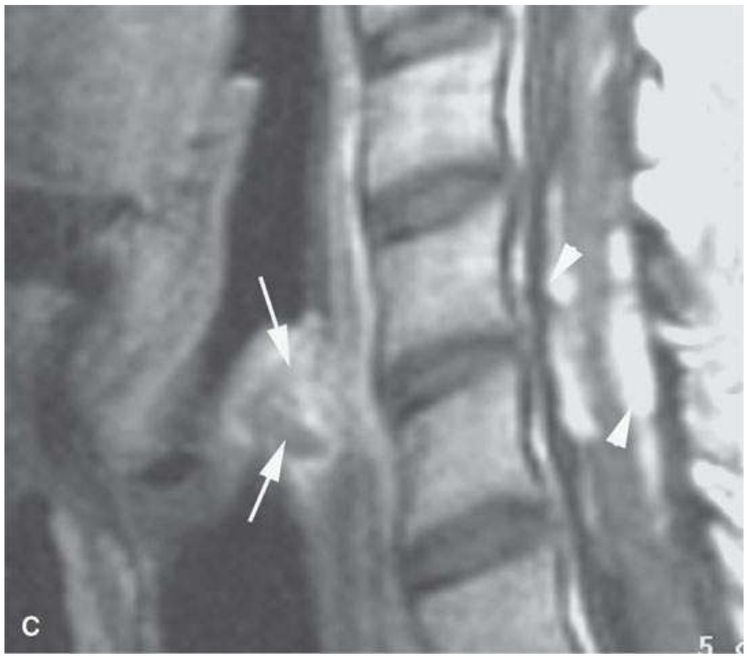
C

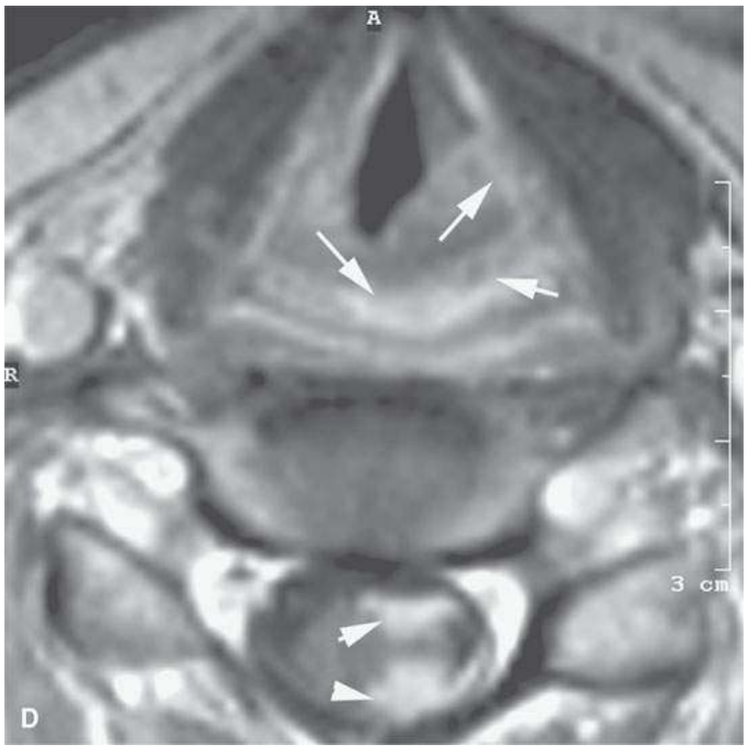

FIGURE 27.23. Magnetic resonance imaging of a patient with central nervous system disseminated non-Hodgkin lymphoma. **A:** Contrast-enhanced T1-weighted (T1W) image showing pia-arachnoid *(arrows)* and dural spread *(arrowhead)*. **B:** Contrast-enhanced T1W image showing continued pia-arachnoid *(black arrow)* and spread "caking" cranial nerves as the course through the medullary cisterns to the jugular fossa *(white arrow)*. **C:** Contrast-enhanced T1W image showing pia-arachnoid "caking" of the spinal cord *(arrowheads)* and spread to the arytenoid pad of the posterior laryngeal wall *(arrows)*. **D:** Contrast-enhanced T1W image correlating with **(C)** showing pia-arachnoid "caking" of the spinal cord *(arrowheads)* and spread to the arytenoid pad of the posterior laryngeal wall *(arrows)*.

Dural and leptomeningeal diseases can present as focal or more diffuse enhancement patterns (Figs. 27.19 and 27.23–27.26). Leptomeningeal disease is usually more prominent within the basilar cisterns and around cranial nerves in the posterior fossa (Fig. 27.23). MRI is far more sensitive than CT for the detection of such meningeal involvement. Dural disease may be seen with or without adjacent bone involvement (Figs. 27.23–27.26).

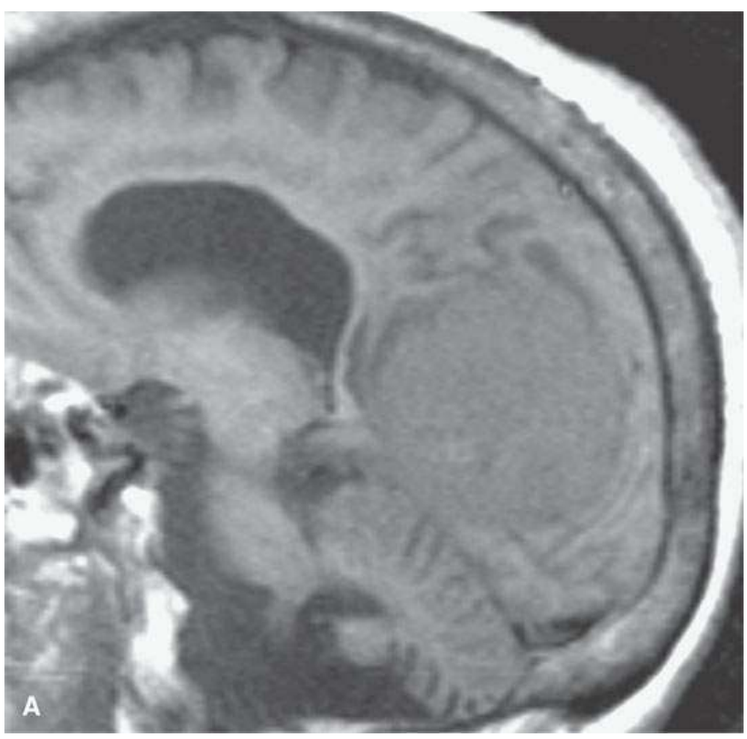

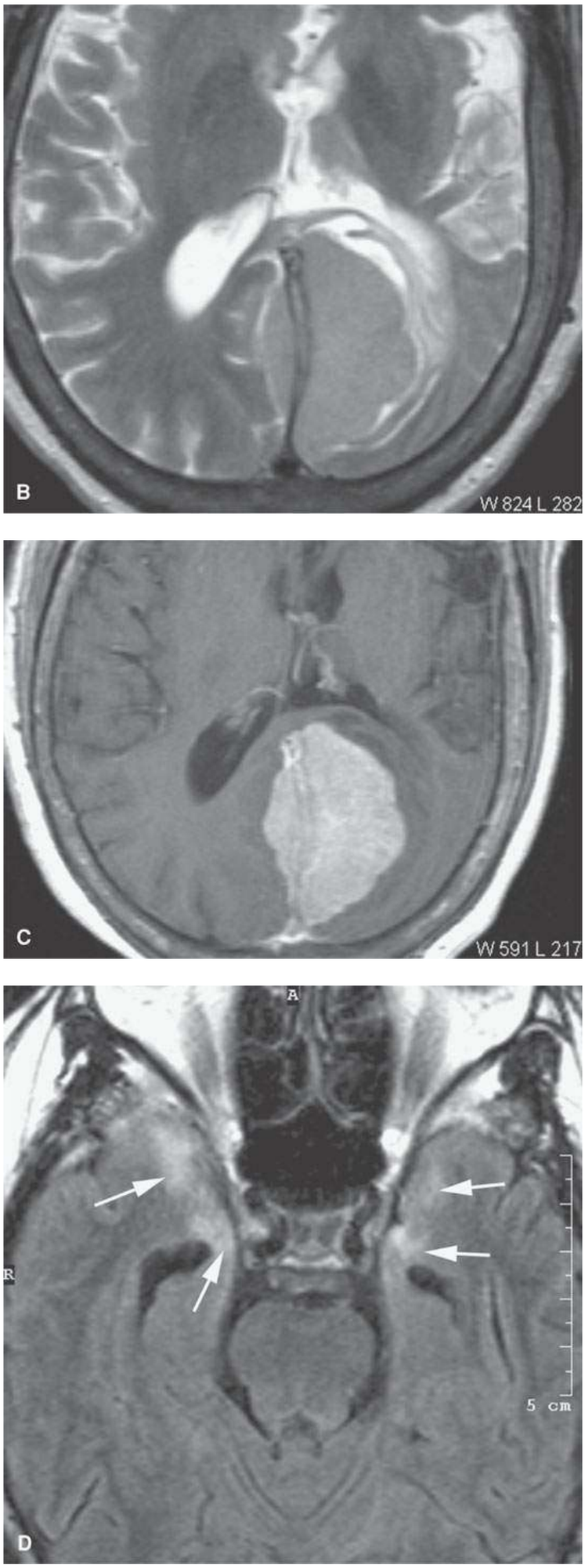

FIGURE 27.24. Magnetic resonance imaging of a patient with central nervous system disseminated non-Hodgkin lymphoma**. A:** Non–contrast-enhanced T1-weighted (T1W) image showing dural mass**. B:** T2-weighted (T2W) image showing the lymphoma to be isointense to gray matter**. C:** Contrast-enhanced T1W image to correlate with **(B)** showing dural mass to enhance quite a bit**. D:** T2W fluid attenuation inversion recovery (FLAIR) image showing the cortical and subcortical effects *(arrows)* of predominantly dural disease**.**

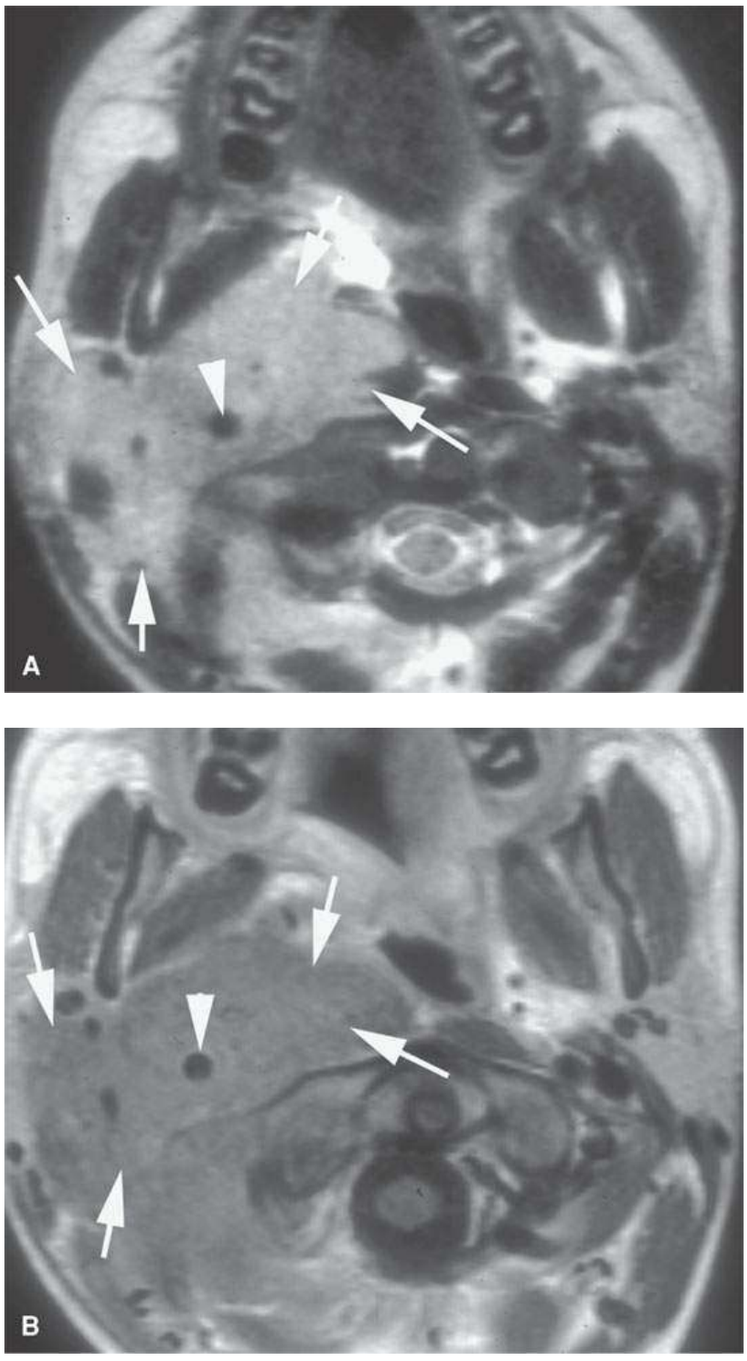

FIGURE 27.25. Magnetic resonance imaging (MRI) of a patient under surveillance following treatment for non-Hodgkin lymphoma.Non–contrast-enhanced T1-weighted image showing lymphoma spreading along the right nerve root sheath *(arrow)* compared to the normal side *(arrowhead)*. (NOTE: Computed tomography and MRI must be searched carefully for evidence of central nervous system disease when being generally evaluated for lymphoma either initially or in surveillance and treatment follow-up.)

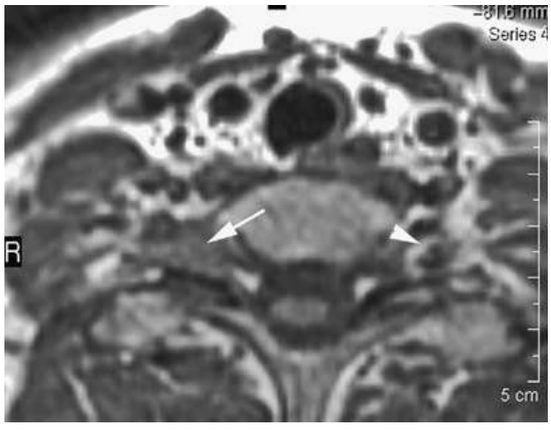

FIGURE 27.26. Magnetic resonance imaging of a child presenting with a neck mass believed to likely be rhabdomyosarcoma with biopsy revealing non-Hodgkin lymphoma. The transcompartmental mass *(arrows)* encases the carotid artery *(arrowheads)*. **A**: T2-weighted image. **B**: Non–contrast-enhanced T1-weighted image.

DIFFERENTIAL DIAGNOSIS

It is impossible to differentiate benign reactive lymphoid proliferations in nodes or at extranodal sites such as the Waldeyer ring from lymphoma on CT, MRI, and ultrasound examinations unless there is invasion of deep tissue planes or some alteration in lymph node architecture such as necrosis or capsular penetration (Figs. 27.18–27.20) or change in vascular pattern as seen on ultrasound (Fig. 26.4 compared to 27.17) suggesting aggressive pathology.14 A large focal accumulation of lymphoid tissue without obvious deep invasion is suspicious in the proper clinical setting but still could be due to local reactive hyperplasia.

Even with imaging morphology suggesting “aggressive behavior,” the proliferation may not be malignant (Chapter 26). Neither MRI signal changes, generalized CT density alterations, nor patterns of contrast enhancement within the lymphoid tissue add unequivocal specificity. This includes patterns that may be observed on contrast-enhanced dynamic flow and perfusion studies. Contrast enhancement only makes it easier to evaluate important gross morphologic features that result in focal nodal defects or invasive character of the extranodal lymphoid proliferation.15

Ultrasound flow patterns, resistive indices, and diffuse architectural nodal changes may be nonspecific in separating reactive proliferative changes from lymphomatous infiltration and other infiltrating pathology such as tuberculosis or squamous cell carcinoma metastatic involvement discussed in Chapters 157 and 158.

Lymphoma involving extranodal sites without an associated obvious pattern of lymphomatous adenopathy in the neck must be distinguished from pseudotumor, plasmacytoma, leukemia, and solid malignant neoplasms such as the fibromatoses and sarcomas that produce local masses that have an infiltrating gross morphology. An infiltrating infectious or noninfectious inflammatory process such as sarcoidosis or Langerhans histiocytosis must also be considered. Destructive vasculitic processes such as Wegener granulomatosis may be entertained as well. Biopsy and appropriate laboratory studies are the only reasonable means of sorting out the cause of the combined worrisome imaging findings and clinical presentation.

TREATMENT

Radiation and chemotherapy are the treatment modalities of choice and are often used in combination. Low-grade lymphoma may be followed without therapeutic intervention.

Suggested Readings

Kim GE, Koom WS, Yang WI, et al. Clinical relevance of three subtypes of primary sinonasal lymphoma characterized by immunophenotypic analysis. *Head and Neck*. 2004;26:(7)584–593.

Ha CS, Medeiros LJ, Charnsangavej C, et al. Lymphoma. *Radiographics*. 2006;26(2):607–620.

Lee HJ, Im JG, Goo JM, et al. Peripheral T-cell lymphoma: Spectrum of imaging findings with clinical and pathologic features. *Radiographics*. 2003;23(1):7–26, discussion 26–28.

Rao DS, Said JW. Small lymphoid proliferations in extranodal locations. *Arch Pathol Lab* Med. 2007;131(3):383–396.

Rodriguez-Vigil B, Gomez-Leon N, Pinilla I, et al. Positron emission tomography/computed tomography in the management of Hodgkin’s disease and non-Hodgkin’s lymphoma. *Curr Probl Diagn Radiol*. 2006;35(4):151–163.

Vega F, Lin P, Medeiros LJ. Extranodal lymphomas of the head and neck. *Ann Diagn Pathol*. 2005;9(6):340–350.

References

1. Leong IT, Fernandes BJ, Mock D. Epstein-Barr virus detection in non-Hodgkin’s lymphoma of the oral cavity: An immunocytochemical and in situ hybridization study. *Oral Surg Oral Med Oral Pathol Oral Radiol Endod*. 2001;92(2):184–193.

2. Zettl A, Lee SS, Rudiger T, et al. Epstein-Barr virus-associated B-cell lymphoproliferative disorders in angioimmunoblastic T-cell lymphoma and peripheral T-cell lymphoma, unspecified. *Am J Clin Pathol*. 2002;117(3):368–379.

3. Suzuki K, Ohshima K, Karube K, et al. Clinicopathological states of Epstein-Barr virus-associated T/NK-cell lymphoproliferative disorders (severe chronic active EBV infection) of children and young adults. *Int J Oncol*. 2004;24(5):1165–1174.

4. Gandhi D, Gujar S, Mukherji SK. Magnetic resonance imaging of perineural spread of head and neck malignancies. *Top Magn Reson Imaging*. 2004;15(2):79–85.

5. Garcia-Serra A, Price Mendenhall N, Hinerman RW, et al. Management of neurotropic low-grade B-cell lymphoma: Report of two cases. *Head Neck*. 2003;25(11):972–976.

6. Salzburg J, Burkhardt B, Zimmermann M, et al. Prevalence, clinical pattern, and outcome of CNS involvement in childhood and adolescent non-Hodgkin’s lymphoma differ by non-Hodgkin’s lymphoma subtype: A Berlin-Frankfurt-Munster Group Report. *J Clin Oncol*. 2007;25(25):3915–3922.

7. Ezzat AA, Ibrahim EM, El Weshi AN, et al. Localized non-Hodgkin’s lymphoma of Waldeyer’s ring: Clinical features, management, and prognosis of 130 adult patients. *Head Neck*. 2001;23(7):547–558.

8. Kim GE, Koom WS, Yang WI, et al. Clinical relevance of three subtypes of primary sinonasal lymphoma characterized by immunophenotypic analysis. *Head Neck*. 2004;26(7):584–593.

9. King AD, Lei KI, Ahuja AT. MRI of neck nodes in non-Hodgkin’s lymphoma of the head and neck. *Br J Radiol*. 2004;77(914):111–115.

10. Gossmann A, Eich HT, Engert A, et al. CT and MR imaging in Hodgkin’s disease—Present and future. *Eur J Haematol Suppl*. 2005;(66):83–89.

11. Beggs I. Primary muscle lymphoma. *Clin Radiol*. 1997;52(3):203–212.

12. Wu CH, Chang YL, Hsu WC, et al. Usefulness of Doppler spectral analysis and power Doppler sonography in the differentiation of cervical lymphadenopathies. *AJR Am J Roentgenol*. 1998;171(2):503–509. Erratum in: *AJR Am J Roentgenol*. 1998;171(5):1428.

13. Yang WT, Chang J, Metreweli C. Patients with breast cancer: Differences in color Doppler flow and gray-scale US features of benign and malignant axillary lymph nodes. *Radiology*. 2000;215(2):568–573.

14. Mancuso AA. Cervical lymph node metastases: Oncologic imaging and diagnosis. *Int J Radiat Oncol Biol Phys*. 1984;10(3):411–423.

15. Smirniotopoulos JG, Murphy FM, Rushing EJ, et al. Patterns of contrast enhancement in the brain and meninges. *Radiographics*. 2007;27(2):525–551.

Related Posts:

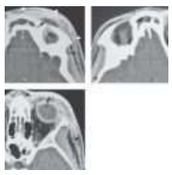

Preseptal Compartment:

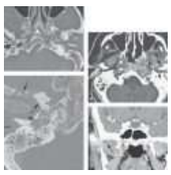

Necrotizing ("Malignant") Otitis

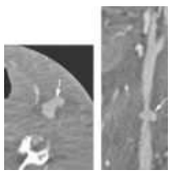

Cervicothoracic Junction: Brachial

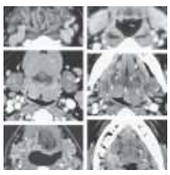

Oropharynx: Introduction

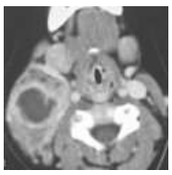

Branchial Apparatus

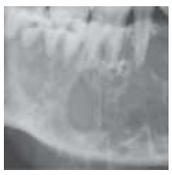

Mandible and Maxilla:

May 14, 2017 | Posted by admin in HEAD & NECK IMAGING | Comments Off